UNIVERSIDADE D
COIMBRA

Diogo António Jarró Margato

Production, characterization and immobilization of bacterial metallophores for the recovery of rare earth metals

Dissertação no âmbito do Mestrado em Bioquímica, orientada pela Doutora Ana Paula Chung e pela Professora Doutora Paula Maria Vasconcelos Morais e apresentada ao Departamento Ciências da Vida da Faculdade de Ciências e Tecnologia da Universidade de Coimbra.

Julho de 2022

Departamento de Ciências da Vida da Faculdade de Ciências e Tecnologia da Universidade de Coimbra

Production, characterization and immobilization of bacterial metallophores for the recovery of rare earth metals

Diogo António Jarró Margato

Dissertação no âmbito do Mestrado em Bioquímica, orientada pela Doutora Ana Paula Chung e pela Professora Doutora Paula Maria Vasconcelos Morais e apresentada ao Departamento Ciências da Vida da Faculdade de Ciências e Tecnologia da Universidade de Coimbra.

Julho de 2022

UNIVERSIDADE D
COIMBRA

ACKNOWLEDGMENTS

This Dissertation for the Master's Degree in Biochemistry at UC is a corollary of all the work carried out over two years in a challenging journey, in which teachers, family and friends contributed and provided very strong support.

I would like to thank my supervisor, Doctor Ana Paula Chung, for always attentive and scientific guidance on this dissertation, which, through her genuine leadership, inspired me with the confidence and spirit to work in a productive and meaningful way. I recognize your ability to analyze deeply and your unique points of view on which my best decisions are based.

I thank Professor Paula Maria Vasconcelos Morais, director of the Laboratory of Microbiology at the University of Coimbra, for giving me the opportunity to develop in this very significant space for my learning. Her commitment and passion for his work motivated me every day. I acknowledge your effort to accompany this journey of mine, an example of respect, ethics and dedication. Her careful scientific co-orientation provided me with greater learning and rigor on this path.

I would like to express my gratitude to the remaining Professors of the Laboratory and to my colleagues, masters and doctoral students, with whom I have been depriving, making my maturity more and more scientific.

I also thank Professor Maria Emília Azenha, for all the support in my learning path in Biochemistry. I recognize his great scientific and work capacity, which has been a permanent incentive for my development.

I would like to thank my family, especially my parents and my brother Rui for their unconditional support in my decisions. To my grandparents, to those who have passed away and to those who are still here with us, for the teachings and love that were the foundation of my life.

INDEX

ABBREVIATIONS

BAM – basal agar medium

BPR – bromopyrogallol red

CAS – Chrome Azurol Sulphonate

DDTC – diethyldithiocarbamate

DFOB – deferrioxamine B

EDC - 1-Ethyl-3-(3-dimethylaminopropyl) carbodiimide

FI – fluorescence intensity

FPLC – Fast Protein Liquid Chromatography

MES - 2-(N-morpholino)ethanesulfonic acid

OD_{600} – Optical Density $\lambda = 600$ nm

PvdI – pyoverdine I

REEs – Rare Earth Elements

RPM – rotations per minute

SDS – sodium dodecylsulfate

RESUMO

Muitas bactérias respondem à escassez de metais no meio ambiente através da produção e libertação de metalóforos, que são metabolitos secundários especializados no sequestro de catiões metálicos, com o objectivo de aumentar a biodisponibilidade desses catiões. A estabilidade dos metalóforos para com os catiões metálicos e a estabilidade do complexo formado depende de diferentes factores, tais como a denticidade e a estrutura do metabolito. Metalóforos hexadentados permitem a formação de complexos hexacoordenados com uma geometria octaédrica com o catião metálico e, por sua vez, metalóforos cíclicos formam complexos ainda mais estáveis que metalóforos lineares, já que aumenta a resistência a enzimas. Estes compostos orgânicos são também capazes de formar complexos com metais terras-raras, porém os valores logarítmicos das contantes de estabilidade entre deferrioxamine B (DFOB) e metais terras-raras são várias unidades inferiores ao valor logarítmico da constante de estabilidade DFOB-Fe^{3+}. O objectivo do presente trabalho consiste na identificação de estirpes bacterianas produtoras de metalóforos do tipo hidroxamato com a finalidade de recuperar metais terras-raras em soluções aquosas, através da ligação destes metais a hidroxamatos imobilizados em partículas magnéticas. Para atingir este objectivo, foi realizado um *screening* de 19 estirpes bacterianas, isoladas de uma estação de tratamento de águas residuais e de minas, para avaliar as respectivas capacidades para quelatar diferentes metais num meio de cultura sólido contendo indicador Chrome Azurol Sulphonate (CAS). Estirpes bacterianas que apresentaram resultados positivos no *screening* foram selecionadas para continuar com o estudo através da optimização de parâmetros de crescimento, nomeadamente a fonte de carbono e a velocidade de agitação para estimular o crescimento bacteriano e a produção de metalóforos. Das 5 estirpes bacterianas (*Ochrobactrum* sp. 5bvl1, *Bacillus altitudinis* 3w19, *Pseudomonas peli* FBO M7 R9A, *Diaphorobacter polyhydroxybutyrativorans* B2A2W2 and *Serratia fonticola* A3-242) capazes de sequestrar metais no meio sólido, *P. peli* FBO M7 R9A and *S. fonticola* A3-242, foram as estirpes que produziram maior quantidade de metalóforos do tipo hidroxamato e catecolato em meio líquido Modi. Na presença de glicerol e glucose, *P. peli* FBO M7 R9A produziu um máximo de 147 e 162 µM de hidroxamatos, respectivamente. Esta estirpe produziu um máximo de 294 e 424 µM de catecolatos, na presença de glicerol e glucose, respectivamente. *S. fonticola* A3-242 produziu diferentes concentrações de metalóforos consoante a velocidade de agitação. A 140 rotações por minuto (rpm), esta estirpe produziu maior quantidade de catecolatos, até um máximo de 124 µM. Quando incubada a 70 rpm, esta estirpe produziu quase exclusivamente hidroxamatos, aproximadamente 2137 µM. A purificação e concentração de metalóforos presentes no meio de cultura foi realizada por Fast Protein Liquid Chromatography (FPLC), utilizando uma mistura de resinas Amberlite XAD-4 e 16. Esta estratégia foi eficaz na purificação de catecolatos produzidos por *P. peli* FBO M7 R9A and *S. fonticola* A3-242, mas nunca foi possível recuperar hidroxamatos. Já que não foi possível purificar metalóforos do tipo

hidroxamato, foi avaliada a capacidade quelante de DFOB comercial em partículas magnéticas com uma superfície altamente carboxilada. Estas partículas magnéticas eram capazes de quelatar a totalidade de catiões Ga^{3+} em solução aquosa. Verificou-se uma redução na capacidade de quelatação do Ga^{3+} utilizando DFOB imobilizado em partículas magnéticas, com uma redução de 77 a 80% na concentração de Ga^{3+}, após 120 minutos de ensaio. Foi avaliada a resposta de fluorescência de metalóforos purificados na presença de diferentes metais, incluindo 6 metais terras-raras como estratégia para avaliar a interação metalóforo-metal. A redução na intensidade de fluorescência é mais significativa quando os metalóforos purificados são incubados na presença de catiões metálicos com um raio iónico semelhante ao do Fe^{3+}. Verificou-se uma redução significativa na intensidade de fluorescência na presença de $Sc^{3+.}$

ABSTRACT

Many bacteria respond to the scarcity of metals in the environment through the production and release of metallophores, which are secondary metabolites specialized in the sequestration of metal cations, increasing their bioavailability. The affinity of metallophores for ions and the stability of the complex formed depend on factors such as their denticity and metabolite structure. Molecules with three bidentate bonds allow the formation of hexa-coordinated complexes with octahedral geometry with the cations, and cyclic metallophores form more stable complexes than linear metallophores by increasing resistance to enzymes. These organic compounds are also capable of complexing rare earth metals, however the logarithmic values of the stability constants between metallophores and rare-earths are several units lower than the stability constant of deferrioxamine B (DFOB)-Fe^{3+}. In the present work, we intended to identify hydroxamate-type metallophore-producing strains in order to recover Rare Earth Elements (REEs) from aqueous solutions through their binding to hydroxamates immobilized on the surface of magnetic particles. To achieve this objective, 19 bacterial strains isolated from a waste water treatment plant and mines were screened in order to assess their ability to sequester different metals in solid culture medium containing the CAS indicator (Chrome Azurol S). Strains that showed a positive result in solid CAS medium were selected to continue this study through the optimization of growth parameters, in particular the choice of carbon sources and agitation that enhance the growth and production of metallophores. Of the five bacterial strains (*Ochrobactrum* sp. 5bvl1, *Bacillus altitudinis* 3w19, *Pseudomonas peli* FBO M7 R9A, *Diaphorobacter polyhydroxybutyrativorans* B2A2W2 and *Serratia fonticola* A3-242) that were able to sequester metals in solid media, *P. peli* FBO M7 R9A and *S. fonticola* A3-242 were the strains that produced the highest amount of hydroxamates and catecholates in Modi liquid medium. In the presence of glycerol and glucose, *P. peli* FBO M7 R9A produced a maximum of 147 and 162 µM of hydroxamates, respectively. This strain produced a maximum 294 and 424 µM of catecholates, in the presence of glycerol and glucose, respectively. *Serratia fonticola* produced different concentrations of metallophores according to the agitation speed. At 140 rpm, this strain produced the highest amount of catecholates, at a maximum concentration of 124 µM, and at 70 rpm it produced almost exclusively hydroxamates, approximately 2137 µM. A strategy of purification of the metallophores present in the culture medium was implemented using Fast Protein Liquid Chromatography (FPLC), with Amberlite XAD-4 and 16 resins. This strategy was effective in the concentration of catecholates produced by *P. peli* FBO M7 R9A and *S. fonticola* A3-242, however it was not possible to recover hydroxamates. Since it was not possible to purify hydroxamate-type metallophores, the chelating capacity of commercial DFOB immobilized on magnetic particles with a highly carboxylated surface was tested. Magnetic particles themselves were able to chelate the entirety of Ga cations in aqueous solution. There was a reduction in the chelation capacity of Ga with

DFOB immobilized on the magnetic particles, with a reduction of 77-80% of the concentration of Ga, after 120 minutes. It was studied the fluorescence response of purified metallophores in presence of different metals, including six rare earth elements, as a strategy to detect metallophores-metal interaction. The reduction in FI is most significant when incubating the purified metallophores with cations with the ionic radius similar to that of Fe^{3+}. Sc was the only REE in which a significant reduction in FI was identified.

1. Metallophores

Most organisms require Iron (Fe) for several metabolic pathways, including protein synthesis which contains a prosthetic group heme, such as cytochrome *c* oxidase, a transmembrane protein complex present in Bacteria, Archaea and mitochondria of Eukaryotes, essential for ATP production in the electron transport chain (Hider *et al.*, 2010). Fe is one of the most abundant elements on Earth, however its bioavailability is low, because the ion Fe^{2+} in its free form is toxic for organisms and Fe^{3+} is insoluble at physiological pH (Holden *et al.*, 2015; Albelda-Berenguer *et al.*, 2019). Many bacteria and fungi can overcome this by producing siderophores, mostly synthesized by non-ribosomal peptide synthetases (Hider *et al.*, 2010). Siderophore is the term associated to metallophores specialized in sequestrum of ferric ions. Therefore, metallophores are all secondary metabolites of low molecular weight (500-1500 dalton), produced by bacteria and fungi in order to chelate Fe^{3+}, but also other trivalent metals such as Co^{3+}, Cr^{3+} and Mn^{3+} and divalent metals, for example, Cd^{2+}, Zn^{2+}, Co^{2+}, Cu^{2+} and Ni^{2+}, present in the environment, making these cations bioavailable (Holden *et al.* 2015; Hofmann *et al.* 2020). There are over 500 types of metallophores that according to their biochemical characteristics and binding moieties, can be divided to three families: hydroxamates, catecholates, and carboxylates (Figure 1).

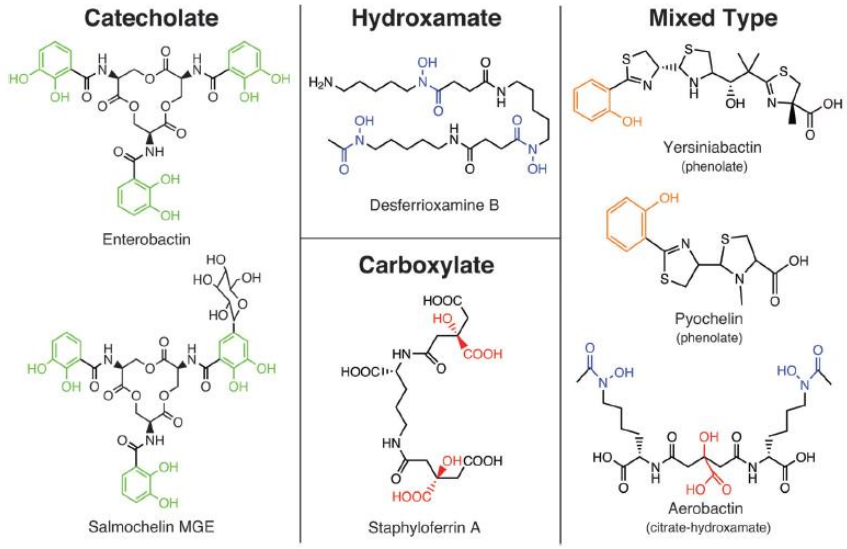

Figure 1 - Metallophores can be divided in three different structural families according to their binding moieties, highlighted in green for catecholate, blue for hydroxamate, and red for carboxylate. Mixed type metallophores contain elements of two or more metallophores families and may also contain phenolate highlighted in orange as a binding moiety. (Adapted from Holden *et al.*, 2015).

Bacterial hydroxamates, such as deferrioxamine B (DFOB), are made up of acylated and hydroxylated alkylamines (Khan *et al,*. 2018). Catecholates, a type of metallophore exclusively produced by bacteria, are lipophilic compounds, resistant to environmental pH variations and made up of dihydroxybenzoic acid (DHBA) coupled to an amino acid (Khan *et al.,* 2018). Carboxylates, which consist of citric acid or β-hydroxyaspartic acid, have carboxyl and hydroxyl groups for metal acquisition (Khan *et al.*, 2018). There are also mixed type metallophores which have elements of two or more metallophore families (Holden *et al.,* 2015). Most metallophores utilize negatively charged oxygen atoms to coordinate with metallic cations, forming complexes (Figure 2). Denticity and structure are factors that influence these secondary metabolites affinity towards metals and the complex stability. Therefore, hexadentate metallophores, like enterobactin and DFOB, which form with ferric ions complexes with an octahedral molecular geometry on a 1:1 stoichiometry, exhibit greater affinity towards these ions in comparison to tetradentate or bidentate metallophores (Hofmann *et al.* 2020). Cyclic metallophores, like enterobactin, form even more stable complexes in comparison to linear metallophores, like DFOB, because cyclization increases both chemical and complex stabilities and resistance to degradation by enzymes (Khan *et al.* 2018). Enterobactin forms the most stable ferric complex amongst all siderophores known, because its size, functional group arrangement and electronic structure are optimal to bind Fe^{3+} (Raymond *et al.* 2015).

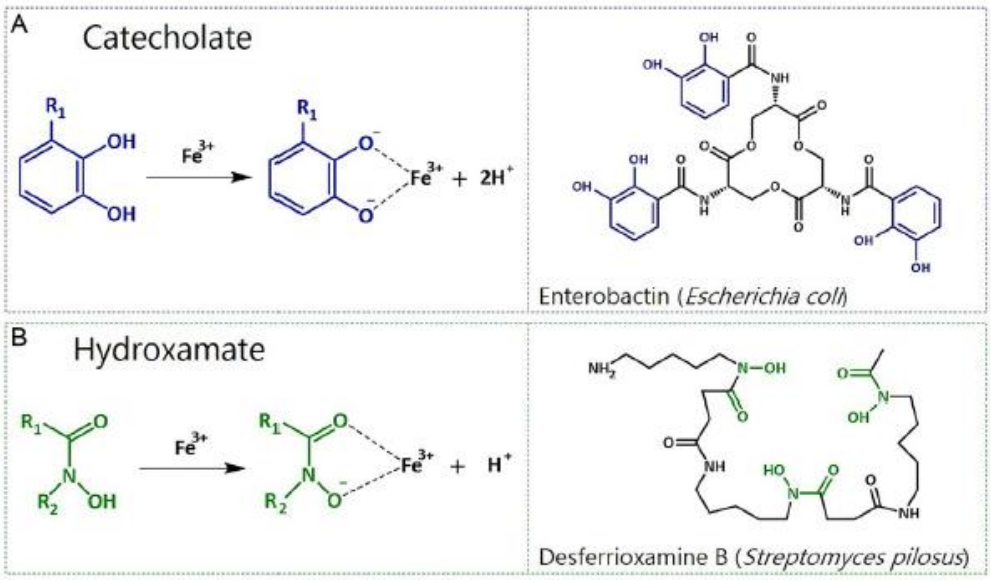

Figure 2 – Negatively charged oxygen atoms present in the binding moieties of catecholate or hydroxamate can coordinate with metal ions, such as Fe^{3+}. (Adapted from Holden *et al*.,2015).

2. Different types of metallophores produced by bacteria

Several bacteria are able to produce different types of metallophores, *Pseudomonas aeruginosa* produces pyoverdine and pyochelin, *Escherichia coli* produces enterobactin and aerobactin, and *Streptomyces coelicolor* produces DFOB and coelichelin, providing an evolutionary advantage for survival in environments contaminated with various metals (Hofmann *et al,*. 2020). Bacteria like *Pseudomonas aeruginosa* PAOI is also able to use the siderophore pyoverdine (PvdI) and the machinery involved in the iron uptake to transport other metals such as Cu^{2+}, Ga^{3+}, Mn^{2+} and Ni^{2+} into the cell but with lower uptake rates (Braud *et al.*, 2009). *Serratia marcescens* is able to produce different types of chatecholates under iron starvation: serratiochelin and the low-affinity siderophore chrysobactin (Weakland *et al.* 2020)

3. Iron uptake by bacteria using siderophores

In Gram-negative bacteria, siderophores are produced and released into the environment, during starvation of ferric ions, and through its high affinity towards these ions, they form soluble ferric complexes which are recognized by specific receptors, present in the outer membrane, and transported into the periplasmatic space (Krewulak *et al.,* 2008). The energy requirement is accomplished through the coupling of the proton motive force of the cytoplasmic membrane to the outer membrane. The complex is then transported by periplasmatic binding proteins and crosses the inner membrane through an ATP-binding cassette (ABC) transporter (Figure 3) (Krewulak *et al.,* 2008). In gram-positive bacteria, the uptake of iron using siderophores involves a membrane-anchored binding protein, which binds to the ferric complex, as well as an ABC transporter (Krewulak *et al.,* 2008).

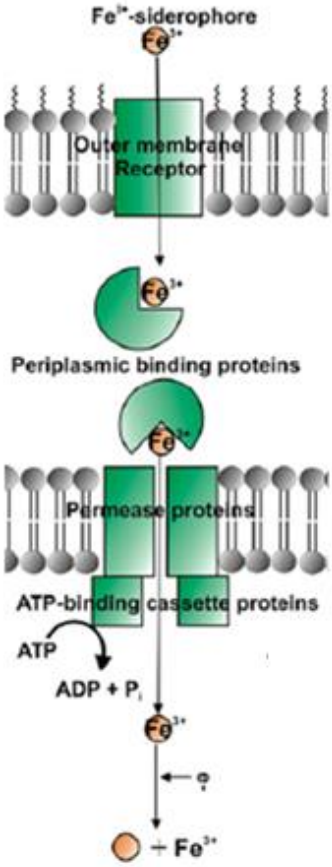

Figure 3 – Schematic representation of iron uptake in Gram-negative bacteria using siderophores. The pathway requires an outermembrane receptor, a periplasmatic binding protein and an inner-membrane ABC transporter. Adapted from (Krewulak *et al.*, 2008)

4. Applications of metallophores

DFOB was the first agent to be used in the treatment of patients with iron overload in the early 1960s. This siderophore had to be administered intravenously due to its low oral availability. However, synthetic iron chelators were developed for clinical use, namely deferiprone (DFP) and deferasirox (DFX), because DFOB is rapidly metabolized and has a short half-life in blood plasma (Kurth *et al.*, 2016). Siderophores can also be conjugated with antibiotics, forming sideromycins, in which the active warhead is covalently linked with a siderophore moiety (Kurth *et al.* 2016). Naturally occurring sideromycins, such as ferrimycin, danomycin and salmycin, can actively bypass membranes to deliver the drug inside the target bacterial cell. During the uptake, the covalent bond is typically cleaved via hydrolysis of an ester or amide bond in the linker region. This 'Trojan horse' strategy can dramatically reduce the inhibitory concentration of an antibiotic, by bypassing bacterial resistance (Kurth *et al.*, 2016).

Metallophores can also be used in biotechnological applications, as a bioremediation tool to remove heavy metal from contaminated soils. Metallophores can solubilize and concentrate heavy metals, which can be separated from the soil matrix (Kurth *et al.* 2016). Diels *et al*. 2021 developed a bioreactor which was able to reduce heavy metals by 16-fold using *Cupriavidus metallidurans*, which produces the metallophore staphyloferrin B. Bacterial siderophores can increase the iron supply of plants, since phytosiderophores might not be sufficient to satisfy the plant's need for Fe in soils contaminated with heavy metals. Some plants are capable to access Fe from complexes formed by bacterial siderophores by direct uptake, chelate degradation or ligand exchange reactions. Such mechanisms also work with metallophores, allowing plants to accumulate different metals. Bioaugmentation of polluted soils with *Ralstonia metallidurans* and *Pseudomonas aeruginosa* increased accumulation of crhomium in maize plants up to 5.4 times (Braud *et al*., 2009).

5. Immobilization of metallophores on surfaces

The amino terminal of DFOB does not participate in the complexation of metal ions, so different strategies have been developed for the immobilization of this metallophore by targeting the N-terminal. Metallophore immobilization on solid supports can be used in different applications (Touma, 2018.) DFOB was immobilized covalently and reversibily on 1 µm aliphatic amine polystyrene beads for the chelation of Fe^{3+}-citrate complexes. The disulfide bond that occurs between DFOB and the beads are readily cleavable upon reduction with dithiothreitol (DTT), allowing the beads to be regenerated and reused. These DFOB-functionalized beads reduced by 51% iron concentrations of solutions from 75 to 37 µM (Touma, 2018). A sensor for Fe^{3+} was developed by coupling DFOB on a self-assembled monolayer on mesoporous silica, in order to study chelation therapy and investigate the half-life of drugs (Biesuz *et al*. 2014). In another study, a colorimetric sensor was developed by functionalizing cellulose filter paper with DFOB for the detection of Fe^{3+} and V^{5+} (Alberti *et al*., 2015). A fertilizing system was proposed by immobilizing DFOB on p-nitrophenylchloroformate activated Sepharose, in order to slowly release iron on deficient crops (Yehuda *et al*., 2012). Kunz and co-workers (2020) immobilized commercial DFOB in magnetic particles with a highly carboxylated surface, and activated it with 1-Ethyl-3-(3-dimethylaminopropyl) carbodiimide (EDC), in order to remove Mn^{2+} from a cellulose pulp. A reduction between 7 and 15% of Mn^{2+} was obtained.

6. Metallophores and Rare Earth Elements

Metallophores have been found to bind REEs. Mohwinkel *et al*. in 2014 were able to chelate 7% of Ce present in trace metals from ocean ferromanganese nodules and crusts. Christenson and co-workers (2011) demonstrated that DFOB can form stable hexadentate coordination complexes with several REEs, whose logarithmic values of the stability constants are from 10 to 15 units, more stable by eight orders of magnitude than complexes between REEs and seawater inorganic compounds, like chloride (Cl^-), sulfate (SO_4^{2-}) and bicarbonate (HCO_3^{2-}). However, these values were far from the logarithmic stability constant of 30 units between DFOB and Fe^{3+} (Winkelmann *et al.*, 1991). Siderophores have extreme selectivity for ferric iron because of its molecular dimensions and the ability to bind Fe^{3+} in its optimal 6-fold coordination. DFOB is a flexible molecule and is able to fold itself around the metal cation, coordinating its three hydroxamate groups, separated by 9 atom spacers, around the ion. Therefore, its central cavity is capable of accommodating ions of different radius, however the more the molecule stretches the smaller is his affinity towards the ion (Christenson *et al.*, 2011).

7. Rare Earth Elements and Circular Economy

REEs are a set of seventeen elements composed of Scandium (Sc), Yttrium (Y) and the fifteen lanthanides (Kurth *et a*l., 2016). Light Rare Earth Elements (LREE), namely Lanthanum (La), Cerium (Ce), Praseodymium (Pr), Neodymium (Nd), Promethium (Pm) and Samarium (Sm) and Heavy Rare Earth Elements (HREE), such as Europium (Eu), Gadolinium (Gd), Terbium (Tb), Dysprosium (Dy), Holmium (Ho), Erbium (Er), Thulium (Tm), Ytterbium (Yb) and Lutetium (Lu), are part of a list of 30 Critical Raw Materials (CRM) essential for European economy (Kinnair *et al.*, 2022). CRMs are particularly important for high tech products and emerging technological innovations. Technological progress and quality of life are reliant on access to a growing number of raw materials (Gauß *et al*., 2021). The world major suppliers are schematized in Figure 4. Most REEs are not particularly rare in terms of abundance, they are widely distributed geographically and there are significant rare earth reserves in Europe. However no mining takes places in Europe, mostly due to environmental challenges from mining these elements (Gauß *et al*., 2021). Despite China owning only one third of the world's REE reserves, China extracts approximately 80% of REEs worldwide and provides 98% of the EU's supply of REE (EIP, 2021).

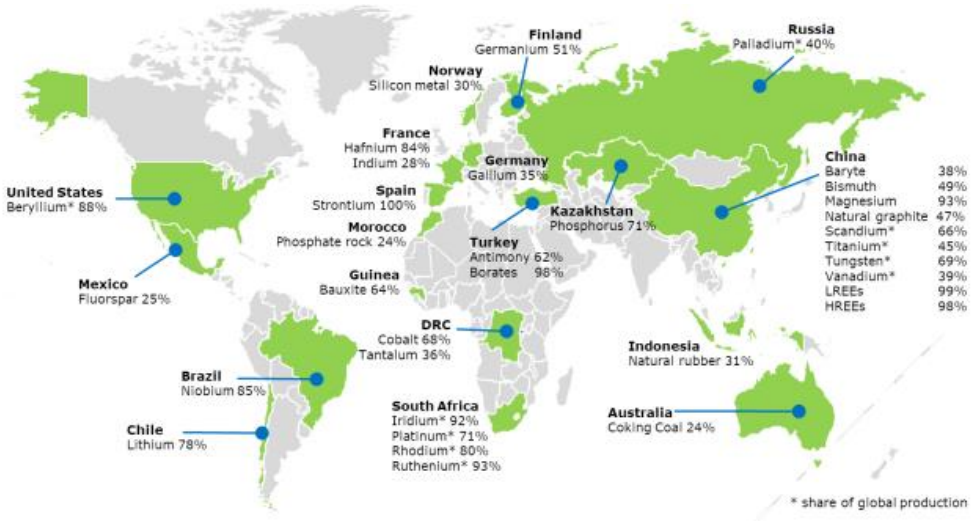

Figure 4 - Major world suppliers of CRMs to the EU. The EU imports from China 99 and 98 % of its LREEs and HREEs, respectively. Adapted from EIP. 2021.

REEs are essential for European economy and transition to green political agenda (Gauß *et al*., 2021). Several properties of these elements, like the magnetic, electronic, optical and even catalytic, have made them an essential resource for many industrial sectors. Such elements are required to produce advanced technology such as the production of magnets for the electronics industry, production of communication devices, production of renewable energy and use in robotics and electric vehicles (Gauß *et al*., 2021). Moreover, the growing demand of the Chinese domestic market for these elements raises major concerns regarding the security of the supply of these resources for European manufacturers. The secure supply of REEs is essential for the competitiveness of European industries, particularly for the development of the "green technology" that require large amounts of these elements (Gauß *et al*., 2021). The European Commission has been promoting the efficient use of resources, as well as encouraging recycling of REEs, with particular emphasis on mining waste and the electronics industry waste. In a circular economy concept (Figure 5) these two kind of wastes are considered a potential secondary source of REEs, which are essential for the production of high-tech equipment, crucial for the competitiveness of the European industry.

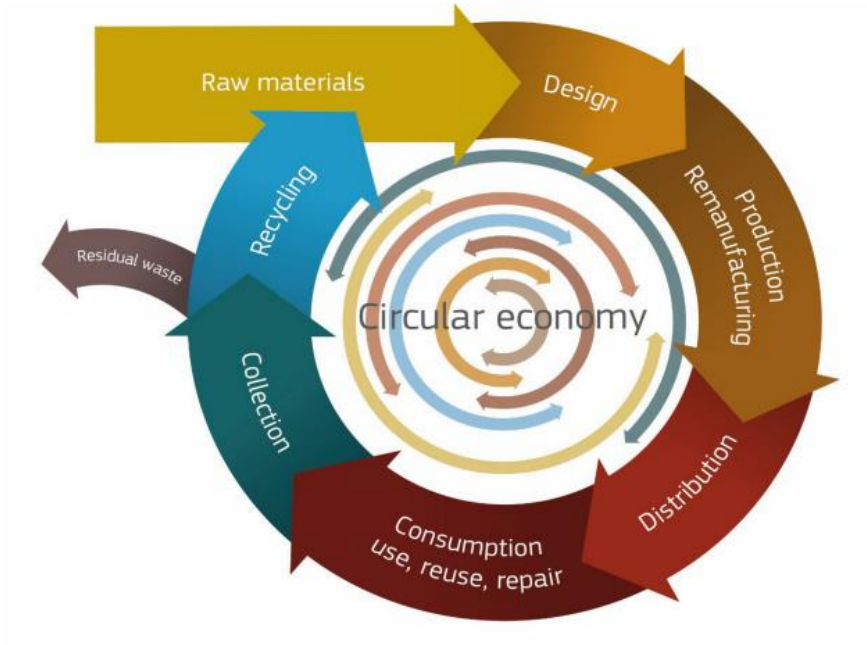

Figure 5 – Diagram illustrating the Circular Economy of raw materials, in particular REE. (Adapted from EIP, 2021)

The development of biotools that are able to recover REEs from secondary resources can contribute to the secure supply of these elements and also to a more environmentally friendly technology than the conventional ones since the use of secondary metabolites as the metallophores does not generate toxic waste products.

OBJECTIVES

The aim of the present work was the identification of bacterial metallophore producers and the determination of optimal parameters for metallophore production. Furthermore, for a selected number of bacterial metallophores with affinity for REEs, several strategies were studied to recover these metals from mixed solutions including the immobilization of these metallophores in magnetic beads and also the evaluation of their fluorescence response in presence of different metals.

In order to achieve these goals, several tasks were completed:

A. Screening for bacterial metallophores producers;
B. Optimization of metallophore production;
C. Biochemical characterization of the metallophores and quantification of the biological production;
D. Metallophore concentration using Amberlite XAD resins and Fast Protein Liquid Chromatography (FPLC);
E. Immobilization of metallophores in magnetic beads for metal removal;
F. Evaluation of the metal binding ability of purified metallophores by competition with Chrome Azurol S (CAS);
G. Study of the fluorescence response of purified metallophores in presence of different metals as a strategy to detect metallophores-metal interaction.

MATERIALS AND METHODS

1. Bacterial strains

A total of nineteen bacterial strains were isolated from metal-stressed environments and were used in this study (Table 1). One of them was isolated from a waste water treatment plant (WWTP) of a leather industry in Alcanena, Portugal. The other eighteen strains were isolated either from a magnesite mine in Spain, or from three different Portuguese mines, a gold mine in Jales, a tungsten mine in Panasqueira and an uranium mine in Urgeiriça.

Table 1 - Bacterial strains used in this study, their respective location of isolation and growth temperature

Isolation local	**Bacterial strain**	**Growth temperature**
Leather industry WWTP Alcanena, Portugal)	*Ochrobactrum* sp. 5bvl1	25°C
Magnesite mine (Navarra, Spain)	*Pseudomonas peli* FBO M7 R9A	30°C
	Sphingopyxis sp. FBO C8 N1.13 B1	30°C
Gold mine (Jales, Portugal)	*Mesorhizobium qingshengii* Ga-15	30°C
	Mesorhizobium qingshengii Te-59	30°C
	Undibacterium sp. W-56	30°C
Tungsten mine (Panasqueira, Portugal)	*Bacillus altitudinis* 3w19	25°C
	Bacillus sp. 5w24	25°C
	Cellulomonas cellasea MPN10	25°C
	Cellulomonas sp. B1 S42.2 2-As4	25°C
	Diaphorobacter polyhydroxybutyrativorans B2A2W2	25°C
	Paenibacillus etheri B1 S5.3.2.10W-5B	25°C
	Paenibacillus lupini B1 S5.4.2.5W-30	25°C
	Priestia aryabhattai B1 S5.4.2.10W27b	25°C
	Rhodanobacter sp. B2A1 Ga-4	30°C
Uranium mine (Urgeiriça, Portugal)	*Arthrobacter silviterrae* A2-55	30°C
	Rugamonas sp. A1-17	30°C
	Serratia fonticola A3-242	25°C
	Sphingomonas sp. A2-49	25°C

2. Screening for bacterial metallophores producers

The bacteria metallophore production capacity was determined in Chrome azurol Sulphonate (CAS) agar medium containing different metals, as described in the literature [12,13]. Briefly, this assay is based on the competition for metals between CAS and the chelating compounds produced by bacteria. Metals are removed from CAS by metallophores that have the highest affinity for the cation. Removal of the metal by the metallophores leads to a change in the color of the solid culture medium.

Twelve different metals were used in the CAS assay, of which 6 were rare earth elements. The metals stock solution were prepared at the following concentration: $FeCl_3$•6H2O (1 mM), $PtCl_4$ (45 mM), $CuSO_4$ (500 mM), $Ga(NO_3)_3$ (200 mM), $InCl_3$ (500 mM), $AlCl_3$ (200 mM), $CeCl_3$ (100 mM), $ScCl_3$•H_2O (100 mM), $NdCl_3$•H_2O (250 mM), $LaCl_3$•$7H_2O$ (250 mM), YCl_3•$6H_2O$ (100 mM), $PrCl_3$•H_2O (200 mM), and were sterilized by filtration using 0.2 µm filters (Sartorius, Germany).

The CAS agar medium was prepared in 3 steps:

a) Preparation of CAS indicator solution

A volume of 40 ml of CAS indicator solution was prepared for each tested metal by adding 16 mL of Cetrimonium bromide (CTAB) solution (729 mg of CTAB in 400 mL of deionized water heated to 50°C), 20 mL of CAS solution (605 mg of CAS in 500 mL of deionized water) and 4 mL of deionized water (except for $FeCl_3$, because it was added 4 mL of its aqueous solution to the CAS indicator). The CAS indicator was sterilized in an autoclave, cooled and the stock metal solutions were added in a sterile environment to make up a concentration of 0.1 mM for each metal.

b) Preparation of the solid culture medium

The culture medium used for the CAS assays was Basal Agar Medium (BAM), which has the following composition, per liter: 30 g 3-(N-morpholino) propanesulfonic acid (MOPS), 0.5 g NaCl, 0.3 g KH_2PO_4, 0.1 g NH_4Cl, 0.5 g DL-asparagine, 0.4 g di-Sodium succinate •$7H_2O$, 1 g mannitol. For 100 ml of CAS agar medium a volume of 88 ml of BAM was prepared and was supplemented with 1.5 g of agar and sterilized in an autoclave.

c) Preparation of CAS Agar plates

A volume of 2 mL of sterilized glucose (50 % w/v) was added to the Basal Agar Medium (prepared in step b) followed by 10 ml CAS indicator solution (prepared in

step a). The resulting 100 ml medium was homogenized and evenly distributed in 4 Petri dishes.

Bacteria that were tested for the ability to produce metallophores were first grown in Reasoner's 2A (R2A) agar medium (VWR CHEMICHALS, Germany) for 72 h, at 25°C or 30°C, according to their growth temperature. Composition of the R2A agar medium, per liter: 0.5 g proteose peptone, 0.5 g tryptone, 0.5 g yeast extract, 0.5 g D(+)-glucose, 0.5 g starch, 0.3 g sodium pyruvate, 0.3 g K_2HPO_4, 0.024 g $MgSO_4$, 15 g agar, pH=7.2 ± 0.2.
The CAS Agar plates were inoculated with 10 µL of bacterial saline suspension and the plates were incubated at the most suitable temperature (25 or 30°C). The bacterial saline suspensions (0.85% NaCl) were prepared with bacterial cultures grown in solid R2A and with a turbidity of 0.05 in the McFarland scale.

3. Optimization of metallophore production

A group of bacteria that were positive in the screening for metallophore production were selected and the parameters for their growth and metallophore production were optimized. The bacteria were grown in modified Modi medium, supplemented with four different carbon sources: glycerol xylose, glucose and arabinose (1 % w/v).
The composition of the modified Modi medium per liter: 0.25 g KH_2PO_4, 0.05 g $MgSO_4 \cdot 7H_2O$, 0.1 g NaCl, 1 g NH_4NO_3, 0.1 g yeast extract, and the final pH was adjusted to 7.0 (Berraho, 1997).
The bacteria were first grown in 100 mL of R2A Broth medium (HiMedia Laboratories, India), the same composition as described in section 2, without the agar, and incubated overnight at the most suitable temperature. The bacterial cultures in R2A were used to inoculate the modified Modi medium.

In a sterile environment, the different carbon sources were added to 100 mL of modified Modi medium, and a volume of the cultures previously grown in R2A was added in order to have an initial Optical Density at 600 nm (OD_{600}) of 0.1 units. Cultures were incubated at 25°C or 30 °C, in an orbital shaker at 70 or 140 rpm. Bacterial growth was monitored periodically by registering OD_{600} and by collecting aliquots of cultures for pH measures and quantification of produced metalophores, namely and hydroxamates and catecholates.

4. Biochemical characterization of the metallophores and quantification of the biological production

The biochemical characterization and the quantification of the produced metallophores was made with wo different colorimetric tests, one proposed by Csaky for the quantification of hydroxamates and the other proposed by Rioux for catecholates.

The Csaky method is based on the oxidation of hydroxylamine to nitrite in acetic acid with iodine and the consequent estimation of the quantification of nitrite after reacting with sulfanilic acid and α-naphthylamine. It consists of adding 100 µL of H_2SO_4 to 100 µL of the supernatant and boil for 10 minutes; cool at room temperature; add 300 µl of 35% Na-acetate, 100 µl of 1% sulfanilic acid in 30% acetic acid and 50 µl of 1.3% sublimed iodine in 100% glacial acetic acid, shake and incubate for 5 minutes at room temperature; then add 100 µl 2% Na-arsenite (0.15 M), 100 µl 0.3% α-naphthylamine in 30% acetic acid and 150 µl deonized water; incubate for 20 minutes at room temperature and measure the absorbance at 526 nm (in the presence of hydroxamates the color of the mixture is pink). The concentration of hydroxamates was extrapolated through a standard curve determined using different concentrations of DFOB (Cśaky, T, 1948).

The Rioux method was used for the quantification of catecholates, which is based on the ability of hydroxyl groups present in aromatic groups to reduce Fe^{3+}, derived from ferric ammonium citrate, to Fe^{2+} in an acid medium. The method consists of adding 460 µl deonized water; 40 µL 20% H_2SO_4; 200 µl supernatant; 20 µL 1 % (w/v) ferric ammonium citrate in 0.09 N H_2SO_4 (fresh reagent); 80 µl 2M ammonium fluoride; 80 µL 1-10 phenanthroline monohydrochloride monohydrate 1% (w/v) in 0.1 N H_2SO_4; 120 µl 3M hexamethylentertamine; then the mixture is heated at 70°C for 1h; cool at room temperature and measure the absorbance at 510 nm (in the presence of catecholates the color of the mixture is orange). The concentration of catecholates was extrapolated through the standard curve determined using different concentrations of dihydroxybenzoic acid (DHBA) (Rioux, C, 1937)

5. Metallophore concentration using Amberlite XAD resins and Fast Protein Liquid Chromatography (FPLC).

The bacterial culture medium supernatants with the produced metallophores were recovered after the removal of cells from the culture medium by centrifugation at 10000 x *g* for 20 minutes.

The metallophores present in the culture medium supernatant were extracted using a 50 ml column packed with a mixture of 45 ml of Amberlite XAD-4 and XAD-16 (in a 1:1 ratio) coupled to a fast protein liquid chromatography (FPLC) device. Amberlite XAD-4 and XAD-16 are non-polar polymeric resins suitable for adsorbing small to medium molecular weight organic substances (metallophores) from aqueous systems and other polar solvents. It is thus possible to separate the components of the mixture since they have different affinities towards the mobile phase and the stationary phase, in this case the resins. The culture medium supernatant is injected through pumps into the column and the metallophores, but also other small peptides, bind to the resin. Other non-polar or high molecular weight components do not bind to the resin. Then, deionized water as mobile phase is used to remove salts that have bound to the resin, and 100 % of methanol is used as elution solution to dissociate metalophores from the resin. This dissociation is monitored by the detector at λ=217 nm, due to the amide bonds of metallophores, and the eluates of interest are collected. In order to evaporate the methanol from the eluates and concentrate the metallophores, a rotary evaporator (HEIDOLPH, Germany) was used and if necessary the samples were also lyophilized to remove remaining water after methanol evaporation. The concentrated solutes were ressuspended in deonized water and the efficiency of metallophore concentration was evaluated by comparing the concentration of hydroxamates (Csaky method) and catecholates (Rioux method) present in the culture medium supernatant with the ressuspended concentrate solutes.

6. Immobilization of metallophores in magnetic beads for metal removal

a. Imobilization of metallophores

Superparamagnetic magnetite beads (M-PVA C22) were purchased from Chemagen Technologies GmbH (CMG-207, PerkinElmer, Baesweiler, Germany). These magnetic beads have a highly carboxylated surface > 950 µmol COOH/g, a concentration of 50 mg/mL, a diameter between 1.0 and 3.0 µm and are designed to bind proteins, nucleic acids or other ligands with amine functionalities.

The most common strategy for attaching proteins or other molecules that contain terminal amine groups to carboxylated particles is through an aqueous process mediated by a carbodiimide, for example 1-ethyl-3-(3-dimethylaminopropyl) carbodiimide hydrochloride (EDC), in a single step reaction. This zero-length bioconjugation reagent is a compound that mediates conjugation between two molecules by forming a bond without the addition of atoms.

This zero-length crosslinker can promote the formation of amide bond between a primary amine and a carboxylic acid and is effective in conjugating a biomolecule into a surface or particle. [20].

In order to immobilize the metallophores produced by our bacteria and also the commercial DFOB to the superparamagnetic magnetite beads the next protocol was followed:

Approximately 7 mg of particles (150 µl of 50 µg/µl) was washed twice with 1 ml of 0.1 M MES buffer, pH 5.3;

These magnetic particles were activated with 1 ml of EDC solution (50 mg EDC in 1 ml MES) and by incubation for 2h on a shaker at 25°C;

The activated particles was washed 3 times with 1 mL MES buffer to remove isourea by-product,

Ligands were immobilized by incubating 1 ml of the saturated solution of DFOB or metallophores (50 mg/ml) with the activated particles, in a shaker at 300 rpm for 18h at 4°C.

After this incubation period, the particles were washed twice with 1 ml of MES buffer and the immobilized DFOB were stored at 4°C [10].

The immobilization of metallophores in magnetic particles is schematized in figure 6

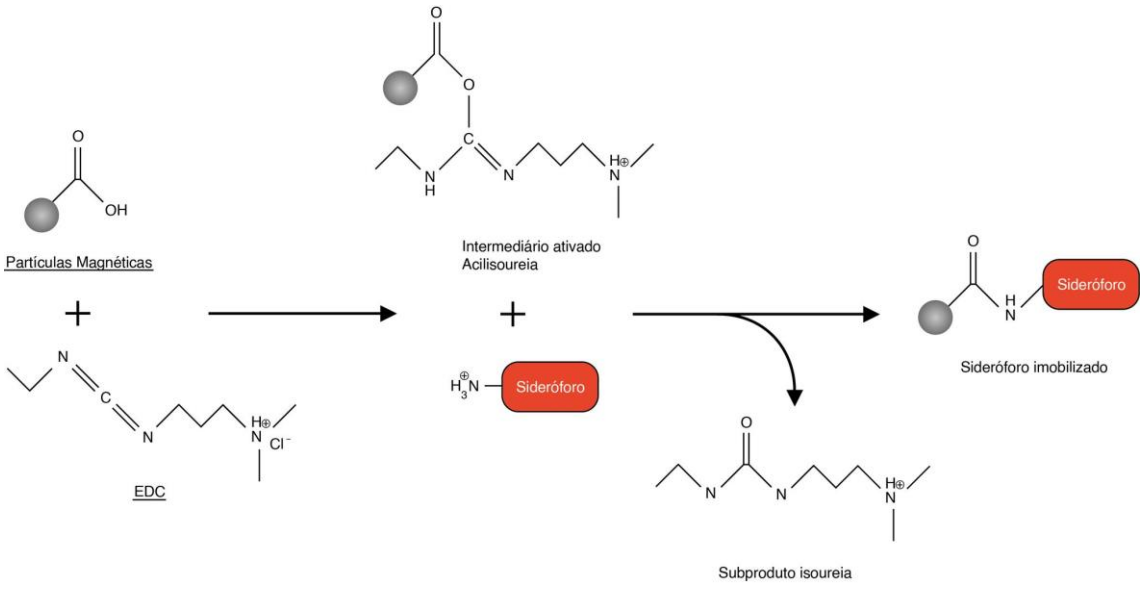

Figure 6 - Activation of magnetic particles using the EDC and immobilization of metallophores on the particles. EDC activates the magnetic particles and allows metallophores to bind to these particles, forming an amide bond between the amine terminal of the metallophores and the carboxylic terminal of the beads

In order to evaluate the binding efficiency of commercial DFOB/produced metallophores to magnetic particles, hydroxamates were quantified before and after incubation of the particles in the DFOB/metallophore saturated solution (50 mg/ml), using the method proposed by Csaky.

b. Metal removal by commercial DFOB immobilized in magnetic particles

The ability of commercial DFOB immobilized on magnetic particles to chelate and remove Gallium (Ga) and copper (Cu) from aqueous solutions was evaluated. The assays consisted of incubating commercial DFOB immobilized on magnetic particles in aqueous solutions of 1 ml of $Ga(NO_3)3$ (1 mM) or $CuSO_4$ (1 mM), at room temperature, 300 rpm, for a period of 120 minutes. Samples were periodically removed and the concentration of these metals was determined. Gallium was quantified by a modification of the bromopyrogallol red (BPR) method (Huang *et al*., 1997), and consisted in mixing, 200 µl of buffer solution (1.25 ml of 0.2 M KCl; 2.65 ml of 0.2 M HCL in 50 ml deionized water), 70 µl of 0.2 % SDS (sodium dodecylsulfate), 100 µl of sample and 200 µl of 0.01% BPR in deionized water to make up a final volume of 1 ml. Samples were quantified spectrophotometrically at 540 nm and the concentration was determined with a calibration curve. Cooper was also quantified spectrophotometrically with diethyldithiocarbamate (DDTC) (Turner *et al*., 1992) and consisted in mixing 800 µL of deionized water, 100 µL of sample and 100 µL of DDTC (0.01 M). Samples were quantified spectrophotometrically at 435 nm and the concentration was determined with a calibration curve.

7. Evaluation of the metal binding ability of purified metallophores by competition with Chrome Azurol S (CAS)

In order to evaluate the metal binding ability of the purified metallophores, CAS assays were performed at the same way as in section 2. The only difference was that the CAS agar plates were inoculated with 10 µL of the concentrated metallophore solution in a 3 mm diameter sterilized paper filter previously placed on the surface of CAS agar. Commercial DFOB (1 mM) was also used as a control of the assays. The inoculated CAS agar plates were incubated at room temperature for 48h. To compare the affinities of the metallophores towards the different

metals, the diameter of the halos formed in solid media were measured and recordered periodically.

8. Study of the fluorescence response of purified metallophores in presence of different metals as a strategy to detect metallophores-metal interaction

The ability of purified metallophores produced by *Pseudomonas peli* FBO M7 R9A and *Serratia fonticola* A3-242, as well as the commercial DFOB, to interact with metals was evaluated by the determination of the fluorescence emission spectra between 250 and 650 nm, when samples were excited at a wavelength of 230 nm, in a spectrofluorometer (infiniteM200, TECAN, Switzerland). The assays were performed in a 96 multiwell plate in a total volume of 200 µL. The acquisition of the fluoresecence emission spectra was made after 5 min., and after 24 h, of interaction between metallophore and metal. An emission spectra of the metallophore without metal, as a control, was always obtained. Eleven of the twelve metals tested in the section 2 were used, namely Fe^{3+}, Pt^{4+}, Cu^{2+}, Nd^{3+}, Y^{3+}, Sc^{3+}, La^{3+}, Pr^{3+}, Al^{3+}, In^{3+} and Ga^{3+}. For each metal 3 different concentration of metals were tested according to the concentration of the metallophore used. *P. peli* FBO M7 R9A metallophore concentration was 345 µM and the different concentrations of metal tested were 125, 250 and 500 µM. *S. fonticola* A3-242 metallophore concentration was 38 µM and the different concentrations of metal tested were 25, 50 and 75 µM. In the case of commercial DFOB, which served for comparative purposes, a concentration of 350 µM was used and the concentrations of metals were 100, 250 and 350 µM.

RESULTS

1. Screening for bacterial metallophores producers

The results of the screening for bacterial metallophores producers are shown in Table 3. Highlighted in blue are bacterial strains that grew in the CAS agar culture medium and formed halos.

Table 3 –Bacterial metallophores producers

		Metals											
Location of isolation	**Bacterial strains**	**Fe**	**Pt**	**Cu**	**Ce**	**Nd**	**Y**	**Sc**	**La**	**Pr**	**Al**	**In**	**Ga**
Leather industry WTP	*Ochrobactrum* sp. 5bvl1	✓/✗	✗/✗	✓/✗	✓/✗	✓/✗	✓/✗	✓/✗	✓/✗	✓/✗	✓/✓	✓/✗	✓/✓
Magnesite mine (Borobia, Navarra)	*Pseudomonas peli* FBO M7 R9A	✗/✗	✗/✗	✗/✗	✗/✗	✓/✓	✗/✗	✓/✓	✓/✓	✗/✗	✗/✗	✗/✗	✗/✗
	Sphingopyxis sp. FBO C8 N1.13 B1	✗/✗	✗/✗	✗/✗	✗/✗	✗/✗	✗/✗	✗/✗	✗/✗	✗/✗	✗/✗	✗/✗	✗/✗
Gold mine (Jales)	*Mesorhizobium qingshengii* Ga-15	✗/✗	✗/✗	✗/✗	✗/✗	✗/✗	✗/✗	✗/✗	✗/✗	✗/✗	✗/✗	✗/✗	✗/✗
	Mesorhizobium qingshengii Te-59	✗/✗	✗/✗	✗/✗	✗/✗	✗/✗	✗/✗	✗/✗	✗/✗	✗/✗	✗/✗	✗/✗	✗/✗
	Undibacterium sp. W-56	✗/✗	✗/✗	✗/✗	✗/✗	✗/✗	✗/✗	✗/✗	✗/✗	✗/✗	✗/✗	✗/✗	✗/✗
Tungsten mine (Panasqueira)	*Bacillus altitudinis* 3w19	✓/✗	✓/✗	✓/✗	✓/✗	✓/✗	✓/✗	✓/✗	✓/✗	✓/✗	✓/✓	✓/✗	✓/✓
	Bacillus sp. 3w24	✗/✗	✗/✗	✗/✗	✗/✗	✗/✗	✗/✗	✗/✗	✗/✗	✗/✗	✗/✗	✗/✗	✗/✗
	Cellulomonas cellasea MPN10	✗/✗	✗/✗	✗/✗	✗/✗	✗/✗	✗/✗	✗/✗	✗/✗	✗/✗	✗/✗	✗/✗	✗/✗
	Cellulomonas sp. B1 S42.2 2-As4	✗/✗	✗/✗	✗/✗	✗/✗	✗/✗	✗/✗	✗/✗	✗/✗	✗/✗	✗/✗	✗/✗	✗/✗
	Diaphorobacter polyhydroxybutyrativorans B2A2W2	✓/✓	✓/✓	✓/✓	✓/✓	✓/✓	✓/✓	✓/✓	✓/✓	✓/✓	✓/✓	✓/✓	✓/✓
	Paenibacillus etheri B1 S5.3.2.10W-5B	✗/✗	✗/✗	✗/✗	✗/✗	✗/✗	✗/✗	✗/✗	✗/✗	✗/✗	✗/✗	✗/✗	✗/✗
	Paenibacillus lupini B1 S5.4.2.5W-30	✗/✗	✗/✗	✗/✗	✗/✗	✗/✗	✗/✗	✗/✗	✗/✗	✗/✗	✗/✗	✗/✗	✗/✗
	Priestia aryabhattai B1 S5.4.2.10W27b	✗/✗	✗/✗	✗/✗	✗/✗	✗/✗	✗/✗	✗/✗	✗/✗	✗/✗	✗/✗	✗/✗	✗/✗
	Rhodanobacter sp. B2A1 Ga-4	✗/✗	✗/✗	✗/✗	✗/✗	✗/✗	✗/✗	✗/✗	✗/✗	✗/✗	✗/✗	✗/✗	✗/✗
Uranium mine (Urgeiriça)	*Arthrobacter silviterrae* A2-55	✗/✗	✗/✗	✗/✗	✗/✗	✗/✗	✗/✗	✗/✗	✗/✗	✗/✗	✗/✗	✗/✗	✗/✗
	Rugamonas sp.A1-17	✗/✗	✗/✗	✗/✗	✗/✗	✓/✗	✗/✗	✗/✗	✓/✗	✗/✗	✗/✗	✗/✗	✗/✗
	Serratia fonticola A3-242	✓/✓	✗/✗	✓/✓	✓/✓	✓/✓	✓/✓	✓/✓	✓/✓	✓/✓	✓/✓	✓/✓	✓/✓
	Sphingomonas sp. A2-49	✗/✗	✗/✗	✗/✗	✗/✗	✗/✗	✗/✗	✗/✗	✗/✗	✗/✗	✗/✗	✗/✗	✗/✗

Subtilte:

✗/✗ - bacteria did not grown or form halo

✓/✗ - bacteria has grown but did not form halo

✓/✓ - bacteria has grown and formed halo

The Gram-negative bacterium *Pseudomonas peli* FBO M7 R9A, isolated from a Magnesite mine, grew in the CAS agar culture medium with three of the six rare earth elements tested, namely Nd, Sc and La, and whenever it grew it also formed large halos (Figure 7), which shows that this strain is capable of producing metallophores that bind these metals.

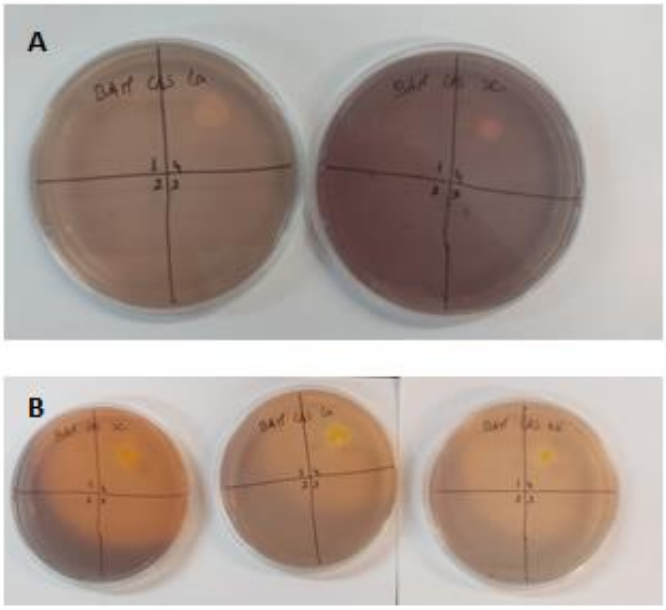

Figure 7 – P. *peli* FBO M7 R9A growth in BAM CAS agar medium containing La and Sc after 6 days (A) and formation of halos after 16 days of inoculation on Sc, La, and Nd (B). Bacterial strains: 1- *Sphingopyxis sp.* FBO C8 N1.13 B1; 2 - *Sphingomonas sp.* A2-49; 3 - *Rhodanobacter sp.* B2A1 Ga-4; 4 - *Pseudomonas peli* FBO M7 R9A.

Ochrobacrum sp. 5bvl1, isolated from a leather industry WWTP, grows in the presence of all tested metals with the exception of Pt. However, this bacterium only forms small halos in the presence of Al and Ga in the culture medium, after 8 days of inoculation (Figure 8). *Bacillus altitudinis* 3w19 a Gram-positive bacterium, isolated from a tungsten mine, showed growth in all tested media after 2 days. However, like strain 5bvl1, it forms only small halos in Al and Ga culture media after 8 days of inoculation.

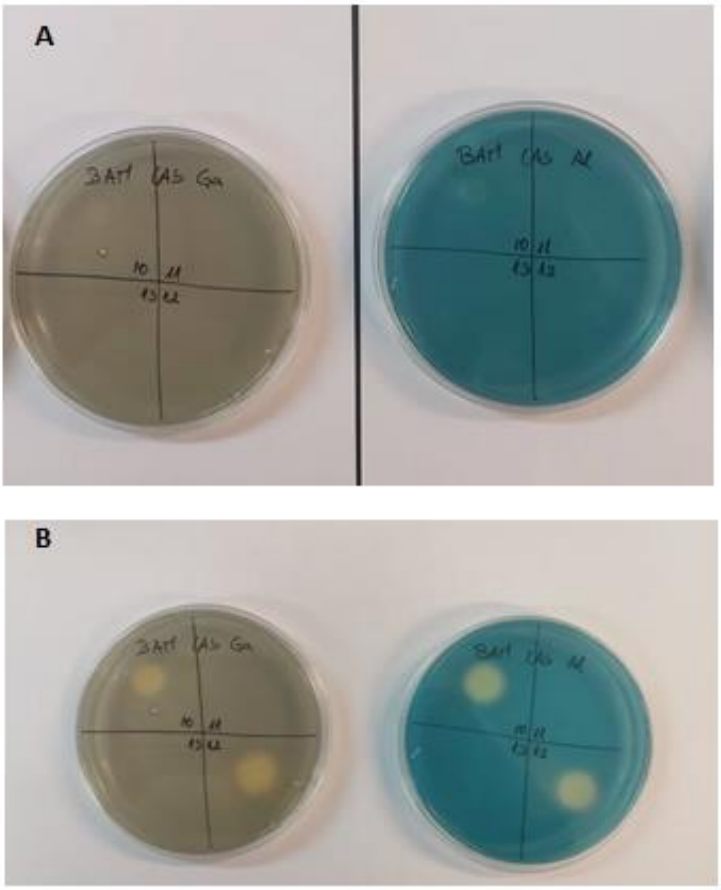

Figure 8 - *Ochrobacrum sp.* 5bvl1 and *Bacillus altitudinis* 3w19 growth and halo formation in BAM CAS agar medium containing Ga and Al, after 2 days (A) and 8 days (B) of inoculation. Bacterial strains: 10 - *Ochrobactrum sp.* 5bvl1; 11 - *Cellulomonas sp.* B1 S42.2 2-As4; 12 - *Bacillus altitudinis* 3w19; 13 – *Bacillus sp.* 5w24.

Diaphorobacter polyhydroxybutyrativorans B2A2W2, isolated from a tungsten mine, grows in all culture media tested after 2 days of incubation and also forms large halos (Figure 9, 10 and 11), which shows that this strain is capable of producing metallophores that bind all tested metals. *Serratia fonticola* A3-242, isolated from an uranium mine is also able to produce metallophores that bind almost all tested metals (Figure 10 and 11). This strain was not able to grow and produce metallophores in CAS medium containing Pt.

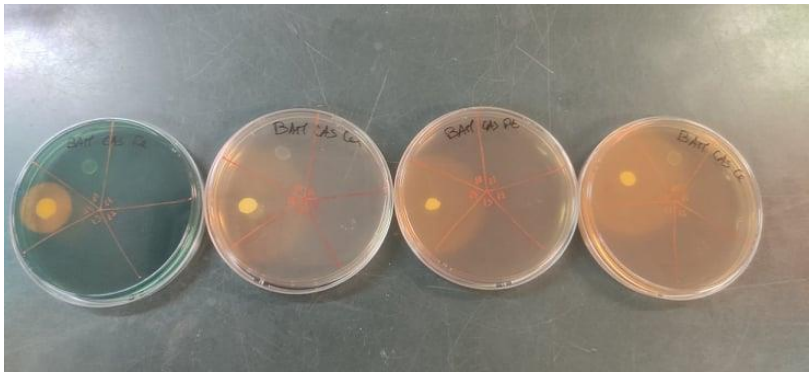

Figure 9 - *Diaphorobacter polyhydroxybutyrativorans* B2A2W2 growth and halo formation in BAM CAS agar medium containing Fe, Cu, Pt and Ce after 10 days of inoculation. Bacterial strains: 10 - *Ochrobactrum sp*. 5bvl1; 11 - *Cellulomonas sp.* B1 S42.2 2-As4; 12 - *Bacillus altitudinis* 3w19; 13 – *Bacillus sp.* 5w24; 14- *D. polyhydroxybutyrativorans* B2A2W2.

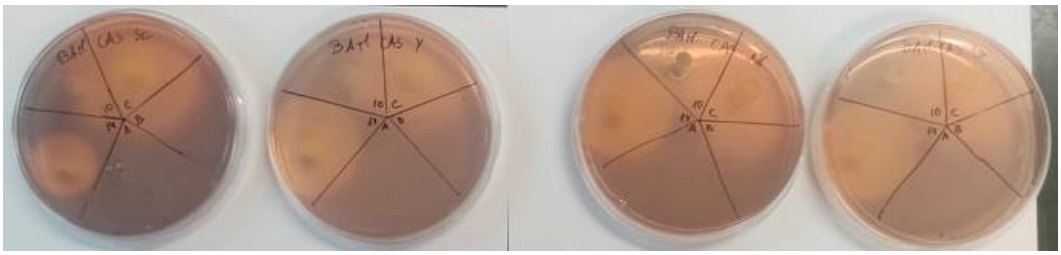

Figure 10 - *Diaphorobacter polyhydroxybutyrativorans* B2A2W2 and *Serratia fonticola* A3-242 growth and halo formation in BAM CAS agar medium containing Sc, Y, Nd and La after 5 days of inoculation.. Bacterial strains: 10 - *Ochrobactrum sp.* 5bvl1; 14 - *D. polyhydroxybutyrativorans* B2A2W2; A - *Arthrobacter silviterrae* A2-55; B - *Priestia aryabhattai* B1 S5.4.2.10W27b; C –*S. fonticola* A3-242.

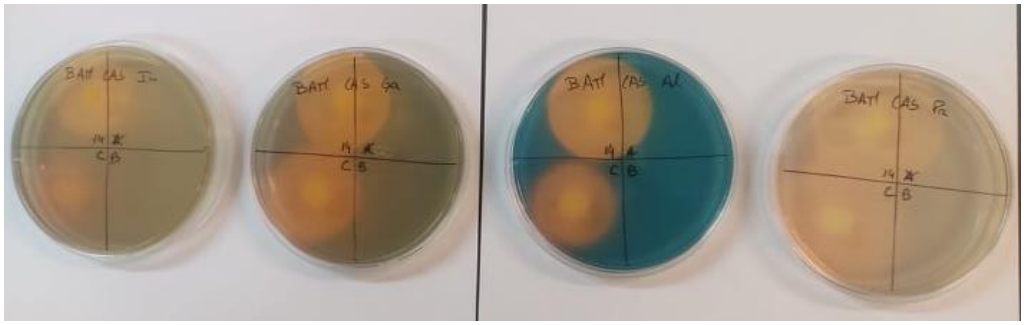

Figure 11 - *Diaphorobacter polyhydroxybutyrativorans* B2A2W2 and *Serratia fonticola* A3-242 growth and halo formation in BAM CAS agar medium containing In, Ga, Al and Pr after 6 days of inoculation. Bacterial strains: 14 – *D. polyhydroxybutyrativorans* B2A2W2; B - *Priestia aryabhattai* B1 S5.4.2.10W27b; C – *S. fonticola* A3-242.

2. Optimization of metallophore production, biochemical characterization and quantification of the produced metallophore

a. *Pseudomonas peli* FBO M7 R9A

The growth of *Pseudomonas peli* FBO M7 R9A was higher in Modi medium supplemented with glycerol or glucose (1 % w/v), reaching on the second day OD_{600} of approximately 3.3 and 2.9 units, respectively (Figure 12). Arabinose is the carbon source that do not favor the growth of this strain, reaching only a maximum of 0.8 units OD_{600}. Growth on xylose was slower, compared to glycerol and glucose, reaching an OD_{600} of 1.7 units on the 19th day. A relationship between bacterial growth and pH variation was identified for this strain. Higher bacterial growth, as in the case of Modi medium with glycerol and glucose, leads to an acidification of the culture medium to pH values of 3 units (Figure 12). In medium with arabinose, the culture medium became more alkaline, with an increase of pH from 6.6 units to 9.0 on the 5th day of incubation. In presence of xylose, an increase of pH to 8.7 units occurred in a first period and after the 5th day there was a decrease of pH to 6.2 units (Figure 12). This strain only produced metallophores of hydroxamates and catecholates type with glycerol and glucose as carbon sources. In presence of glycerol and glucose, the concentration of hydroxamates at the 5th day of growth was 147 and 162 µM, respectively. *P. peli* produced a maximum of catecholates 294 and 424 µM, in presence of glycerol and glucose respectively. The production of these two types of metallophores in the presence of arabinose and xylose was not identified, although bacterial growth was observed in the presence of these carbon sources, mainly in the case of xylose.

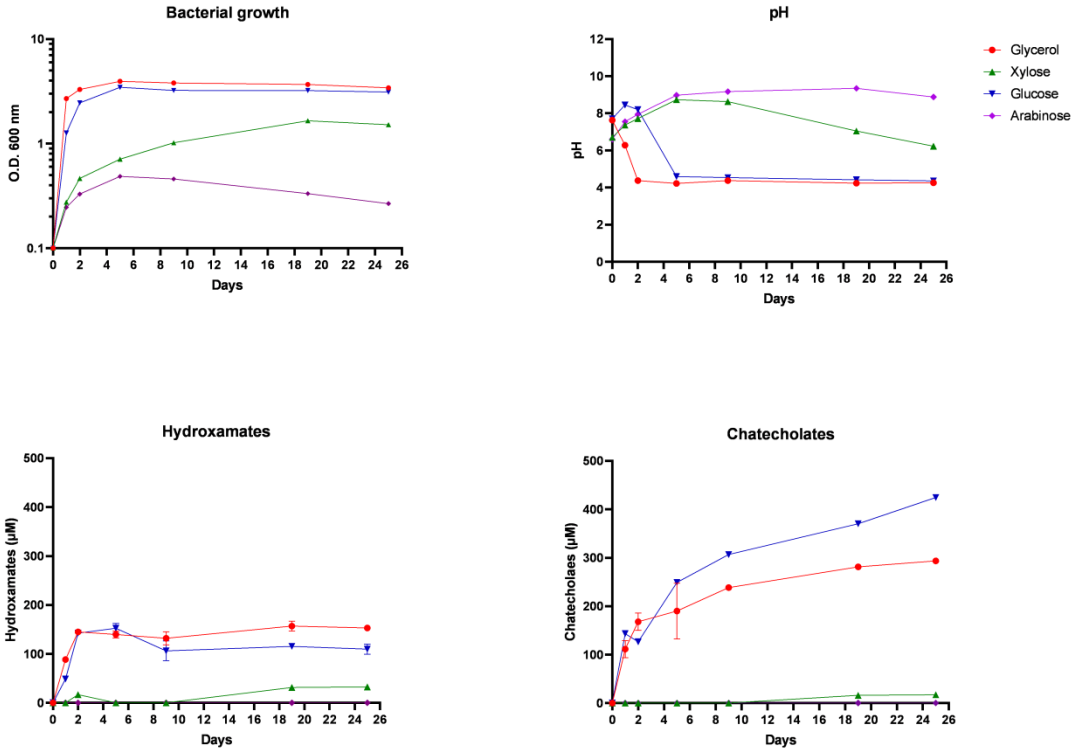

Figure 12 – Growth curves, pH variation, and quantification of hydroxamates and chatecholates of growth cultures of *Pseudomonas peli* FOB M7 R9A in Modi medium with 4 different carbon sources, at the temperature of 25°C and rotary speed of 140 rpm.

b. *Serratia fonticola* A3-242

Serratia fonticola A3-242 was grown at two different rotation speeds 70 and 140 rpm, both at 25°C. At 140 rpm, the bacterial growth of this strain reaches a maximum OD_{600} of 2.2 units in Modi medium supplemented with of xylose (Figure 13). However, all the other carbon sources promoted the growth of this strain. The pH of the culture medium in all four different carbon sources acidifies around 1 unit. This strain does not produce hydroxamates in the presence of xylose and produces a maximum of 45 µM hydroxamates, in Modi medium with glucose, on the 5th day. This strain produces significantly more chatecholates than hydroxamates, at 140 rpm (Figure13). On the second day, the strain produces 107 and 109 µM chatecholates in the presence of arabinose and xylose, respectively. A maximum of 124 µM of cathecholates were produced by this strain n Modi medium in the presence of arabinose. The least favorable carbon source for chatecholate production is glucose, reaching a maximum of 42 µM on the 2nd day of growth.

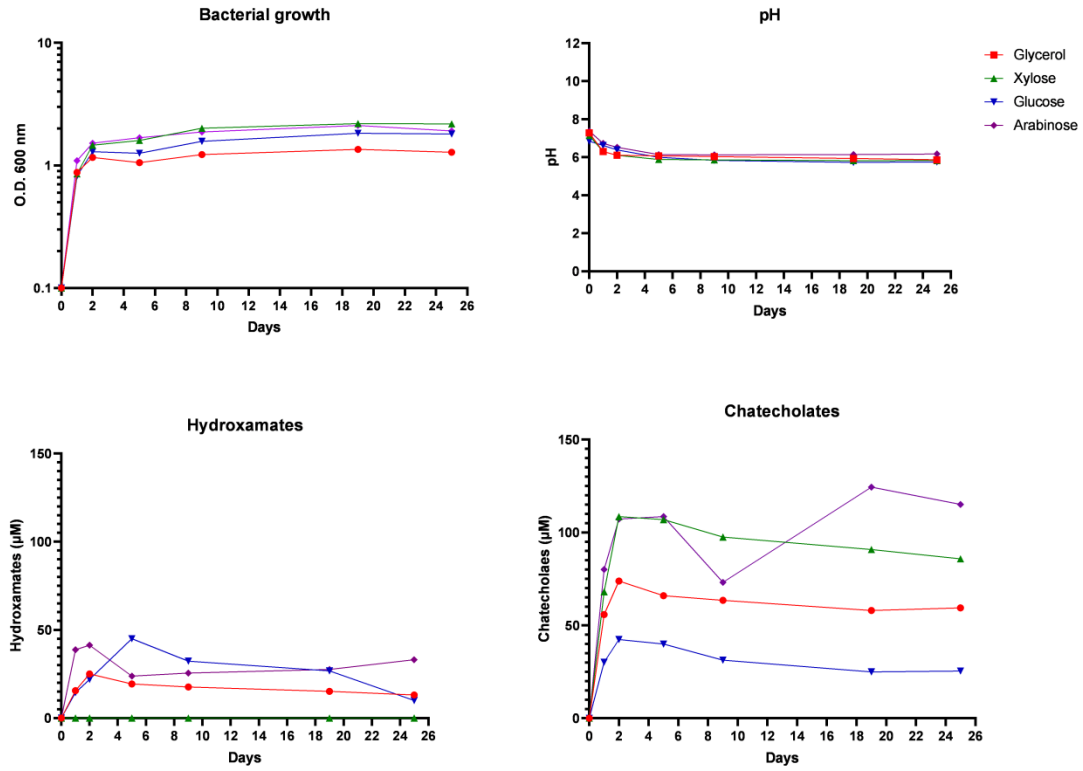

Figure 13 - Growth curves, pH variation, and quantification of hydroxamates and chatecholates of cultures of *Serratia fonticola* A3-242 in Modi medium with 4 different carbon sources, at the temperature of 25°C and rotary speed of 140 rpm.

When *Serratia fonticola* A3-242 was grown with a rotary speed of 70 rpm, the bacterial growth was reduced when compared with 140 rpm (Figure 14). However, this lower rotary speed was used to promote the production hydroxamates, and only glycerol and arabinose were used in the growth medium. In the presence of glycerol, this strain reaches a maximum OD_{600} of 0.447 units, and with arabinose in the medium, reaches a maximum OD_{600} of 0.532. The pH of the culture media decreases to around 6.5 and 6.7 units, in the presence of glycerol and arabinose, respectively. In the presence of glycerol, this strain produces a maximum 2137 µM of hydroxamates, on the 1st day of incubation, and in the presence of arabinose, hydroxamate concentration reaches a maximum of 1812 µM, on the 2nd day of incubation. At 70 rpm, the chatecholate production is either absent in the presence of glycerol or is strongly reduced with a maximum of 22 µM, in the presence of arabinose (Figure 14).

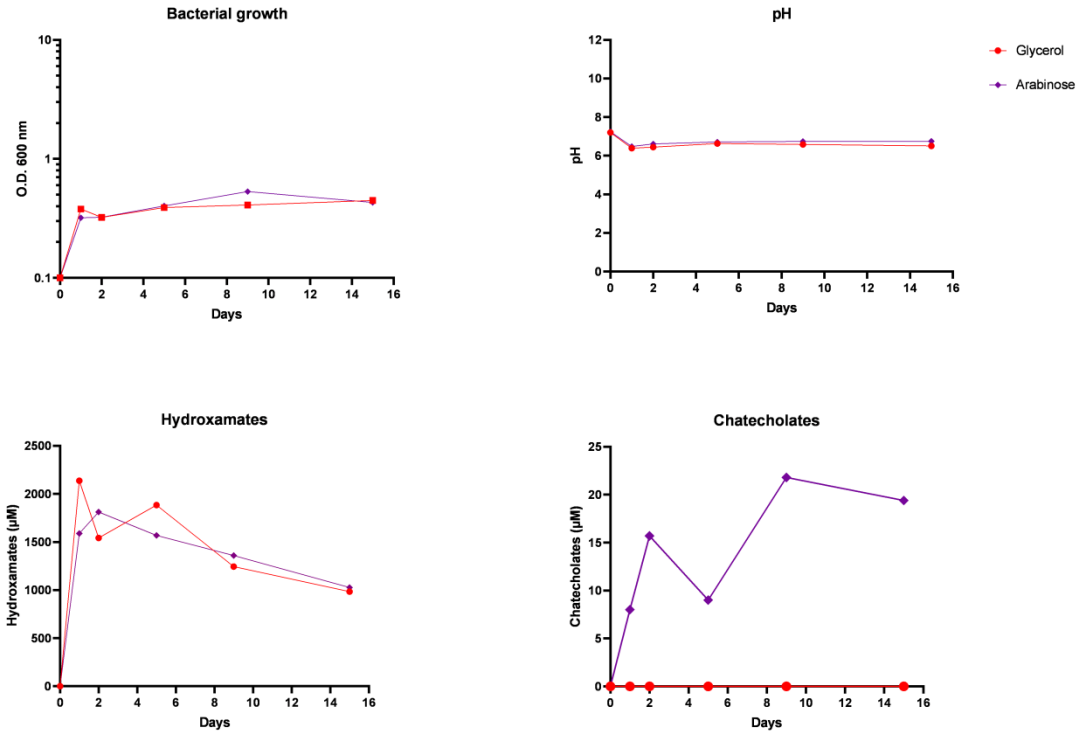

Figure 14 - Growth curves, pH variation, and quantification of hydroxamates and chatecholates of cultures of *Serratia fonticola* A3-242 in Modi medium with 2 different carbon sources, at the temperature of 25°C and rotary speed of 70 rpm.

c. *Diaphorobacter polyhydroxybutyrativorans* B2A2W2

The carbon sources that most favored the growth of *Diaphorobacter polyhydroxybutyrativorans* B2A2W2 were glycerol and glucose, reaching a maximum OD_{600nm} of 3.8 units in glycerol and 2.8 units in glucose (Figure 15). As with the growth of *P. peli*, there is a relationship between bacterial growth and pH variation. The pH of the growth medium decreases to values of 3 units, when this strain has a high bacterial growth. When bacterial growth is lower, the pH of the medium becomes more alkaline, reaching values of 9 units. The quantification of hydroxamates was not possible, probably due to an interference of components resulting from the metabolism of the strain present in the supernatant. The samples instead of showing the usual pink color, showed an orange one. Strain B2A2W2 is a producer of catecholates, it produces a maximum of 387 and 392 µM in presence of glycerol and glucose, respectively.

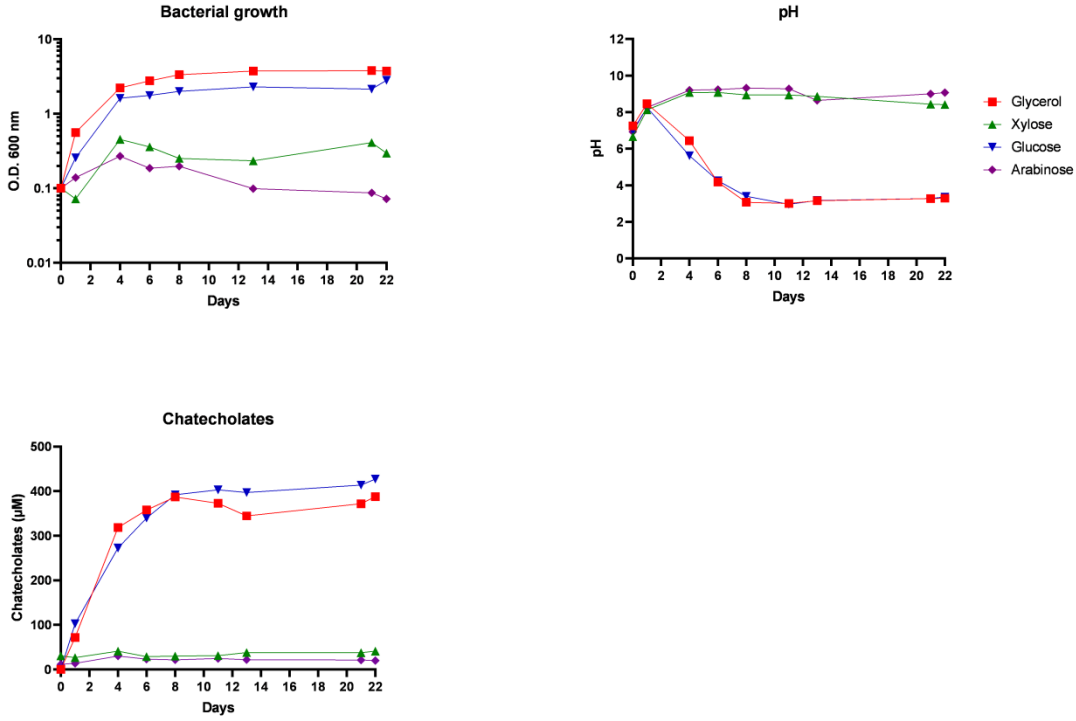

Figure 15 - Growth curves, pH variation, and quantification of hydroxamates and chatecholates of cultures of *Diaphorobacter polyhydroxybutyrativorans* B2A2W2 in Modi medium with 4 different carbon sources, at the temperature of 25°C and rotary speed of 140 rpm.

3. Metallophore purification and concentration

For both bacterial strains *Pseudomonas peli* FBO M7 R9A and *Serratia fonticola* A3-242**,** the metallophore production was made in 300 ml of Modi medium with glycerol as carbon source. The cultures were incubated at 25°C in a rotary shaker at 140 rpm, for a period of 4-5 days. The supernatant of culture medium of *P. peli* FBO M7 R9A exhibited 74 µM of hydroxamate-type metallophore and 196 µM of catechol-type metallophore. However, the supernatant of culture medium of *S. fonticola* A3-242 only showed the presence of catechol-type metallophore in a concentration of 67,9 µM and no hydroxamates were quantified. After the process of purification and concentration the metallophores of *P. peli* FBO M7 R9A, was ressuspended in 6 ml of deionized water. The efficiency of the concentration process was about 70,4 % and the final concentration of the recovered cathecol-type metallophore was approximately 6900 µM. No hydroxamate-type metallophore was recovered from the culture medium. The purified and concentrated cathecol-type metallophore of *S. fonticola* A3-242 was also ressuspended in 6 ml

of deionized water. The efficiency of the concentration process was lower 46,3 %, and the final concentration of recovered cathecol-type metallophore was approximately 1572 µM.

Serratia fonticola A3-242 was grown in 100 ml of Modi medium with glycerol or arabinose as carbon sources and a rotary speed of 70 rpm, to promote the production of hydroxamates for a period of 6 days. The culture media supernatants had 1304 and 1204 µM of hydroxamates, in glycerol and arabinose, respectively, and no catechol-type metallophore was quantified. After the process of purification and concentration, no hydroxamate-type metallophore was recovered. It was found that these type of metallophores do not bind to the mixture of Amberlite resins XAD-4 and 16 and were not eluted by methanol as mobile phase. The process of production of hydroxamate-type metallophore was repeated in Modi medium with glycerol in the same conditions as reported before. After 24 h of growth 1551 µM of hydroxamates and no catecholates was quantified. The process of concentration in FPLC was carried out and this time the aqueous eluate was collected, about 75 ml volume. This aqueous solution had 1155 µM of hydroxamates. After lyophilization to remove water and resuspension of the concentrated hydroxamate-type metallophore in 4 mL of deionized water, the quantification showed a loss in hydroxamate and only 136 µM was present.

4. Immobilization of metallophores in magnetic beads for metal removal

Since it was not possible to purify and concentrate the hydroxamate-type metallophores produced by our bacteria we used commercial DFOB to immobilize in magnetic beads and tested their metal removal capacity.

The magnetic beads were immobilized with two different concentrations of DFOB, a saturating concentration of 50 mg/ml and 15 mg/ml. The efficiency of the immobilization was determined by quantification of the remaining DFOB in solution after removal of the magnetic beads with the immobilized DFOB. The efficiency of the immobilization was 39.9 % for DFOB 50 mg/ml and 19.8% for DFOB 15 mg/ml.

Both magnetic beads with immobilized DFOB was used to remove Ga^{3+} and Cu^{2+} from 1 mM aqueous solutions of $Ga(NO_3)3$ and $CuSO_4$, respectively. Two negative controls was simultaneously used in the assays, the magnetic beads and the magnetic beads activated with EDC. An unexpected result was obtained, the magnetic beads alone was able to chelate and remove all of the metal present in solution within 5 minutes. Regarding the Ga^{3+} chelation assays with DFOB immobilized on magnetic particles and EDC-activated particles, the results are shown in the Figure 16.

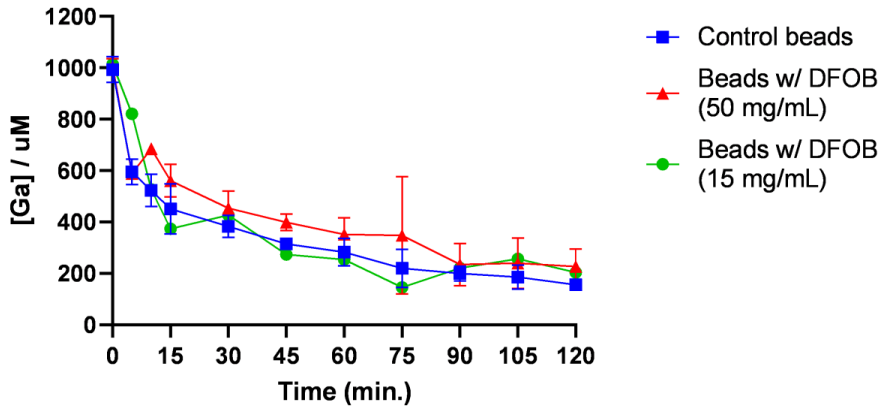

Figure 16 –Gallium removal by activated beads with EDC (control) and by DFOB immobilized in magnetic beads. Beads were incubated with DFOB either at a concentration of 50 or 15 mg/mL.

In the case of the control, the EDC activated beads reduced the concentration of Ga to 450 µM, showing a reduction to 45.4% of the initial concentration, in the first 15 minutes. At the end of 120 minutes, the metal concentration was about 155 µM, which corresponds to reduction of 84.3%. The beads previously incubated with 50 mg/mL of DFOB reduced the metal concentration to 561 µM, about 43.9 % of reduction after 15 minutes. After 120 minutes, Ga concentration was about 226 µM, metal concentration was reduced in 77.8 %. For beads previously incubated with 15 mg/mL of DFOB, the concentration of Ga after 15 minutes was 373 µM, the metal concentration was reduced 61.2 %, and after 120 minutes 203 µM of Ga was present and 80 % of reduction was observed. The percentage of Ga reduction with time is very similar in the 3 assays.

5. Evaluation of the metal binding ability of purified metallophores by competition with Chrome Azurol S (CAS)

The metal binding ability of the purified metallophores and also of the commercial DFOB was evaluated by the formation of halos on the CAS agar culture medium. The diameter of the halos formed by 10 µL of DFOB (1 mM) and the purified metallophores from *P. peli* FBO M7 R9A (6.9 mM) and *S. fonticola* A3-242 (1.5 mM) are described in the tables 4, 5 and 6, respectively.

Table 4 – Diameter of the halos (mm) formed by 10 µL of DFOB (1 mM) in CAS agar culture medium with 12 different metals.

Metal / Time	Pr	Y	Nd	Sc	La	Ce	Fe	Ga	In	Cu	Al	Pt
24h	23	23	23	23	23	23	15	15	24	25	15	23
48h	27	27	27	27	27	27	15	15	27	27	15	27

Table 5 – Diameter of the halos (mm) formed by 10 µL of metallophore (6.9 mM) produced by *P. peli* FBO M7 R9A in CAS agar culture medium with 12 different metals.

Metal / Time	Pr	Y	Nd	Sc	La	Ce	Fe	Ga	In	Cu	Al	Pt
24h	31	30	28	28	31	30	24	24	30	30	24	29
48h	38	39	32	32	36	39	26	25	35	34	26	37

Table 6 - Diameter of the halos (mm) formed by 10 µL of metallophore (1.5 mM) produced by of *S. fonticola* A3-242 in CAS agar culture medium with 12 different metals.

Metal / Time	Pr	Y	Nd	Sc	La	Ce	Fe	Ga	In	Cu	Al	Pt
24h	14	14	15	15	15	14	10	10	15	17	8	15
48h	17	17	16	15	16	18	10	10	15	18	8	19

Three different metallophores with different concentrations were used, they diffused through the solid medium chelating the metals and forming halos, mainly during the first 24 hours. This assay confirmed that the purified metallophores from *P. peli* FBO M7 R9A and *S. fonticola* A3-242 maintained their chelating properties. It is possible to separate the 12 metals into 2 groups according to the size of the halos formed by the DFOB and the metallophores of the two strains. A group constituted by Fe, Ga and Al, in which the three metallophores formed halos with smaller diameter and another group in which the metallophores formed larger halos, which includes the six REEs, In, Cu and Pt.

6. Study of the fluorescence response of purified metallophores in presence of different metals as a strategy to detect metallophores-metal interaction

a) Commercial DFOB

Commercial DFOB in a concentration of 350 µM shows a fluorescence emission spectrum with a peak of maximum fluorescence at 325 nm. The emission spectra of DFOB with 350 µM of Sc showed a reduction in the fluorescence intensity (FI) of 95.4 % at 325 nm (Figure 17). In presence of Y and La the reduction in the FI was not so high, approximately 31.0 and 16.1%, respectively. A shift in the maximum peak of FI to 335 nm was identified with 100 and 250 µM of Sc, however, this shift is not observed at the higher concentration of Sc tested (350 µM). In presence of Pr and Nd, the reduction of FI DFOB was negligible. Nonetheless, a 15.7% increase in FI was observed with 250 µM of Nd (Figure 17). For the remaining metals tested, the presence of 350 µM of metal led to a high reduction in FI, with 3 metals causing an almost total reduction, 98.9% for Pt, 96.7% for In, 94.1 % for Fe (Figure 18). In the presence of Ga, Cu and Al a reduction of approximately 82% was observed. With metals such as Sc, Fe and Ga, a gradual decrease in FI was observed with increasing metal concentration. With Y, Cu and Al, a reduction in FI was observed with 100 µM and 250 µM of metal, however, there is no further significant reduction with 350 µM of metal. In the case of In and Pt, an almost total reduction was observed in the intermediate metal concentration. In general, there was no changes between the emission spectra obtained after 5 minutes and 24 hours of incubation (Figure 17 and 18).

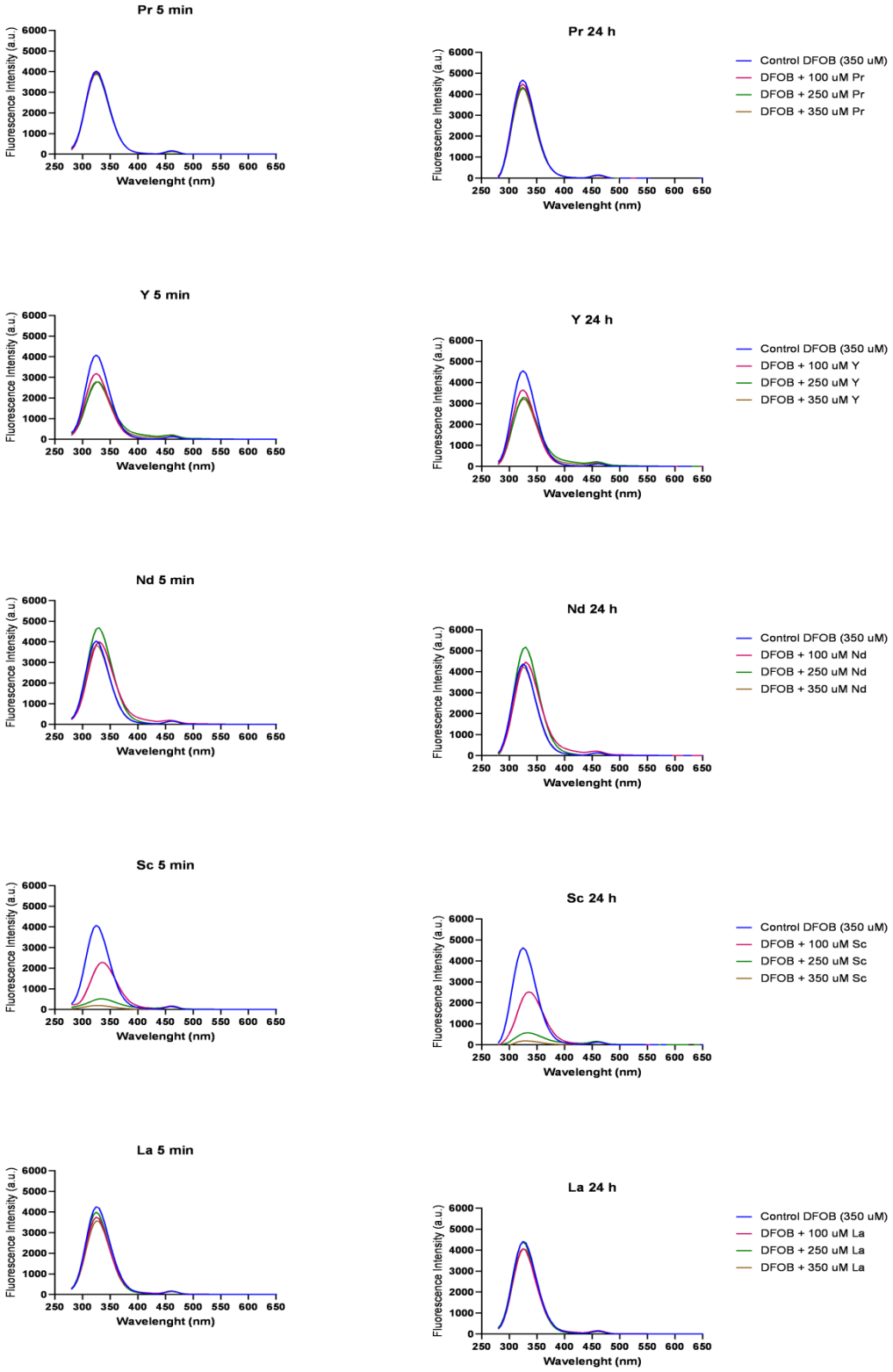

Figure 17 – Fluorescent emission spectra of DFOB incubated in the presence of 5 rare earth elements. Three different concentrations of each rare earth were used and the fluorescent emission spectra were obtained after 5 minutes and 24 hours of incubation at room temperature.

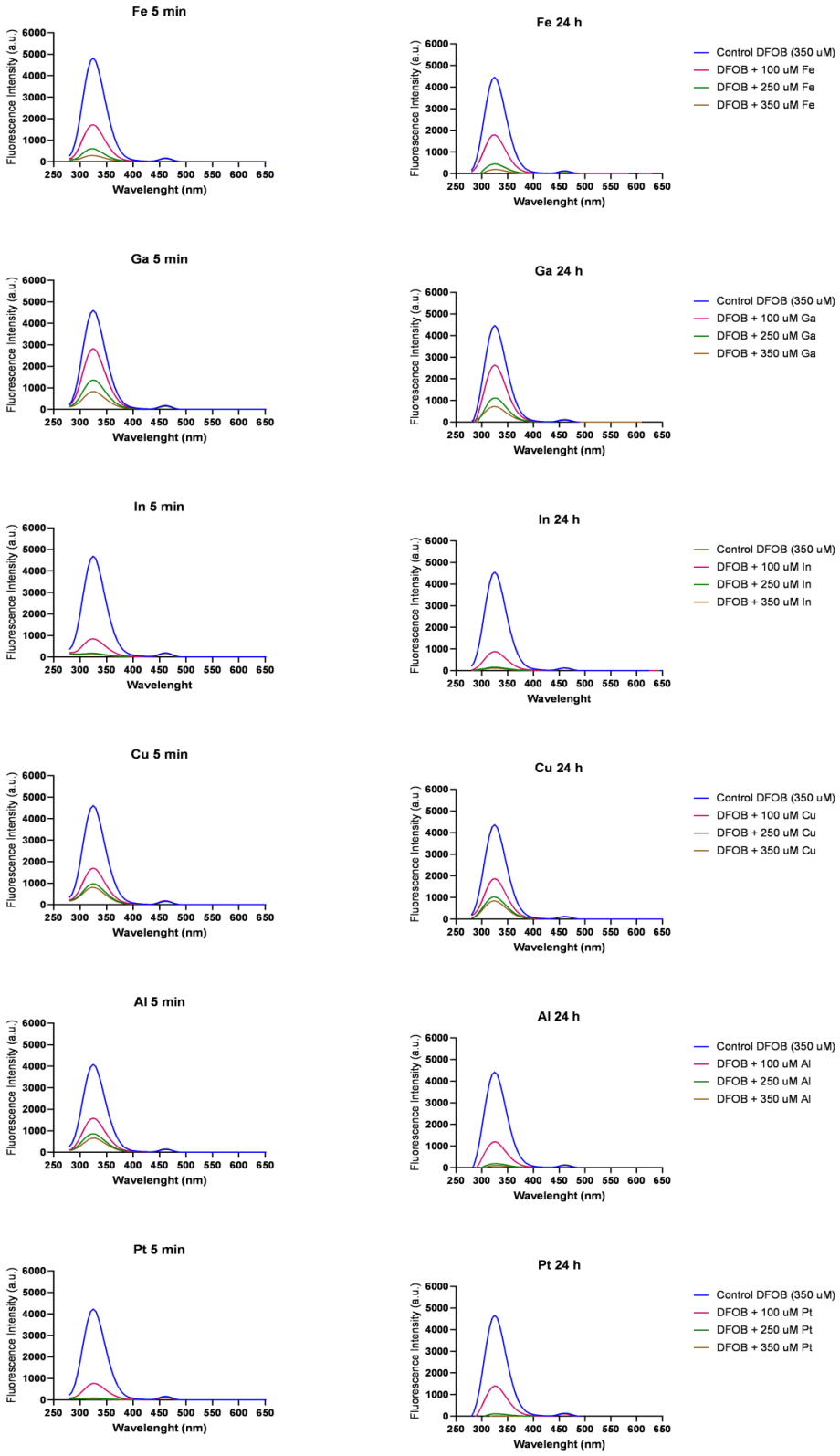

Figure 18 - Fluorescent emission spectra of DFOB incubated in the presence of 6 different metals. Three different concentrations of each metal were used and the fluorescent emission spectra were obtained after 5 minutes and 24 hours of incubation at room temperature.

b) *P. peli* FBO M7 R9A

Cathecol-type metallophore purified from *P. peli* FBO M7 R9A with a concentration of 345 µM shows a fluorescence emission spectrum with 2 maximum fluorescence peaks, one between 350 and 355 nm and the other between 450 and 455 nm (Figure 19 and 20). Regarding rare earth elements, changes in fluorescence intensity (FI) were only observed in Sc. The emission spectra obtained after 5 minutes of incubation with 125 and 250 µM of Sc, showed a reduction in FI of the first peak and an increase in the FI of the second peak. With 500 µM Sc, both peaks showed a reduction in FI, 49.5 % for the first peak and 23.8 % for the second peak (Figure 19). The spectra obtained at 24 h in presence of Sc, was different from the one obtained at 5 minutes, with no increase in fluorescence observed in the second peak and a decrease in FI with increasing metal concentration was also observed. In the case of Fe and Ga, this trend was also observed, a gradual reduction in FI with increasing metal concentration. The fluorescence emission spectra with 500 µM of these two metals showed a reduction in FI of 43.7% and 47.8% in the first and second peaks, respectively (Figure 20). There were no significant changes in the 24-hour spectra of these two metals. In the case of In, at 5 minutes the FI is very similar in the 3 different concentrations of metal, with a reduction of approximately 33% over all spectra. In the 24-hour spectrum with 125 µM of In there is an increase in the FI of the first peak. With Cu, the FI is similar with 250 and 500 µM of metal. For Al, the FI in the first peak is similar at 250 and 500 µM and there are no significant changes in the FI in the second peak, relative to the control. With Pt, in the 5-minute spectra, a gradual reduction in FI is observed with increasing metal concentration and it is possible to identify a reduction of 67.3 and 51.7 % in FI in the first and second peaks of the 500 µM spectrum. In the 24-hour spectra the second peak has similar FI at the three different metal concentrations (Figure 20).

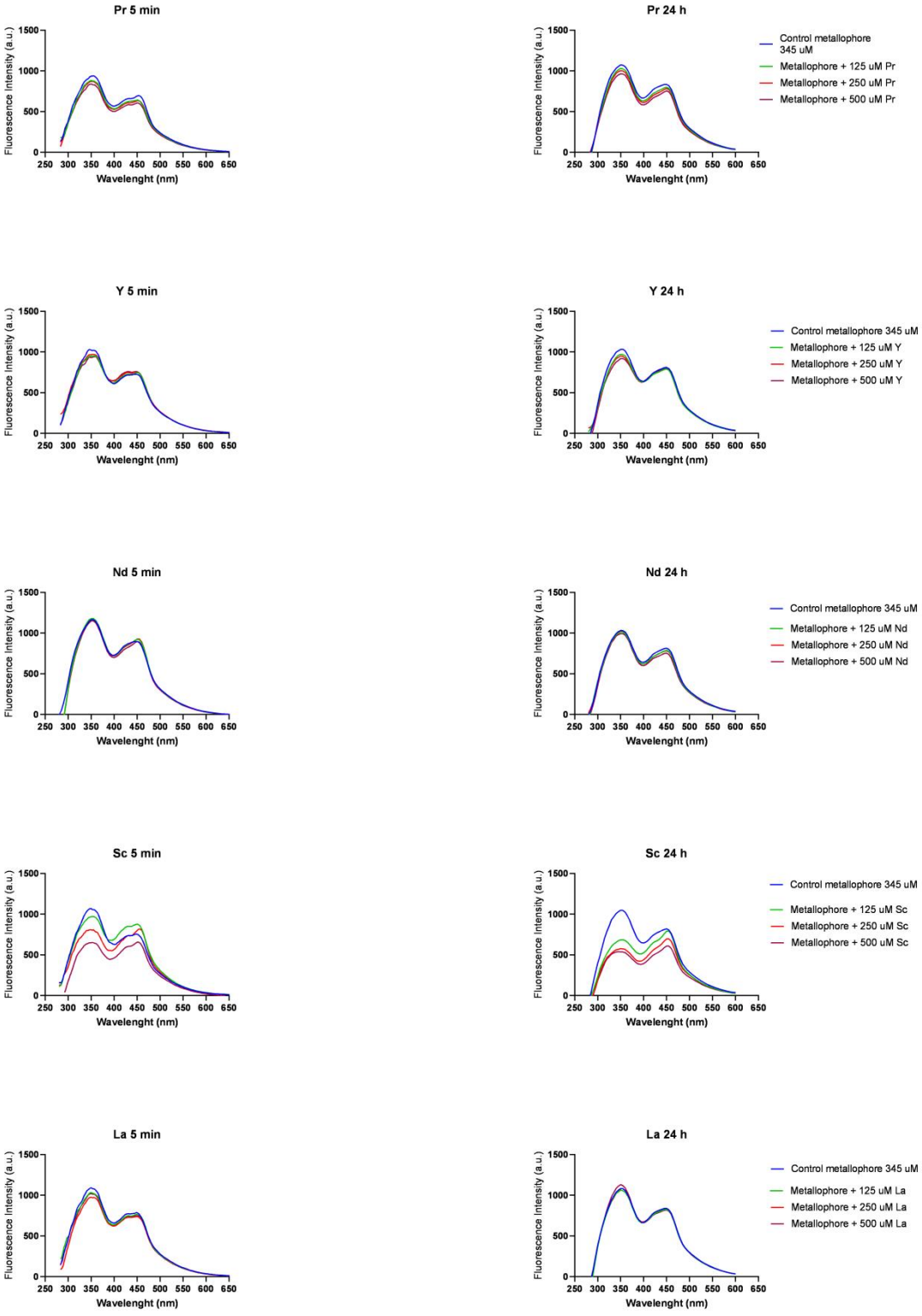

Figure 19 - Fluorescent emission spectra of metallophore produced by *P. peli* FBO M7 R9A incubated in the presence of 5 rare earth elements. Three different concentrations of each rare earth element were used and the fluorescent emission spectra were obtained after 5 minutes and 24 hours of incubation at room temperature.

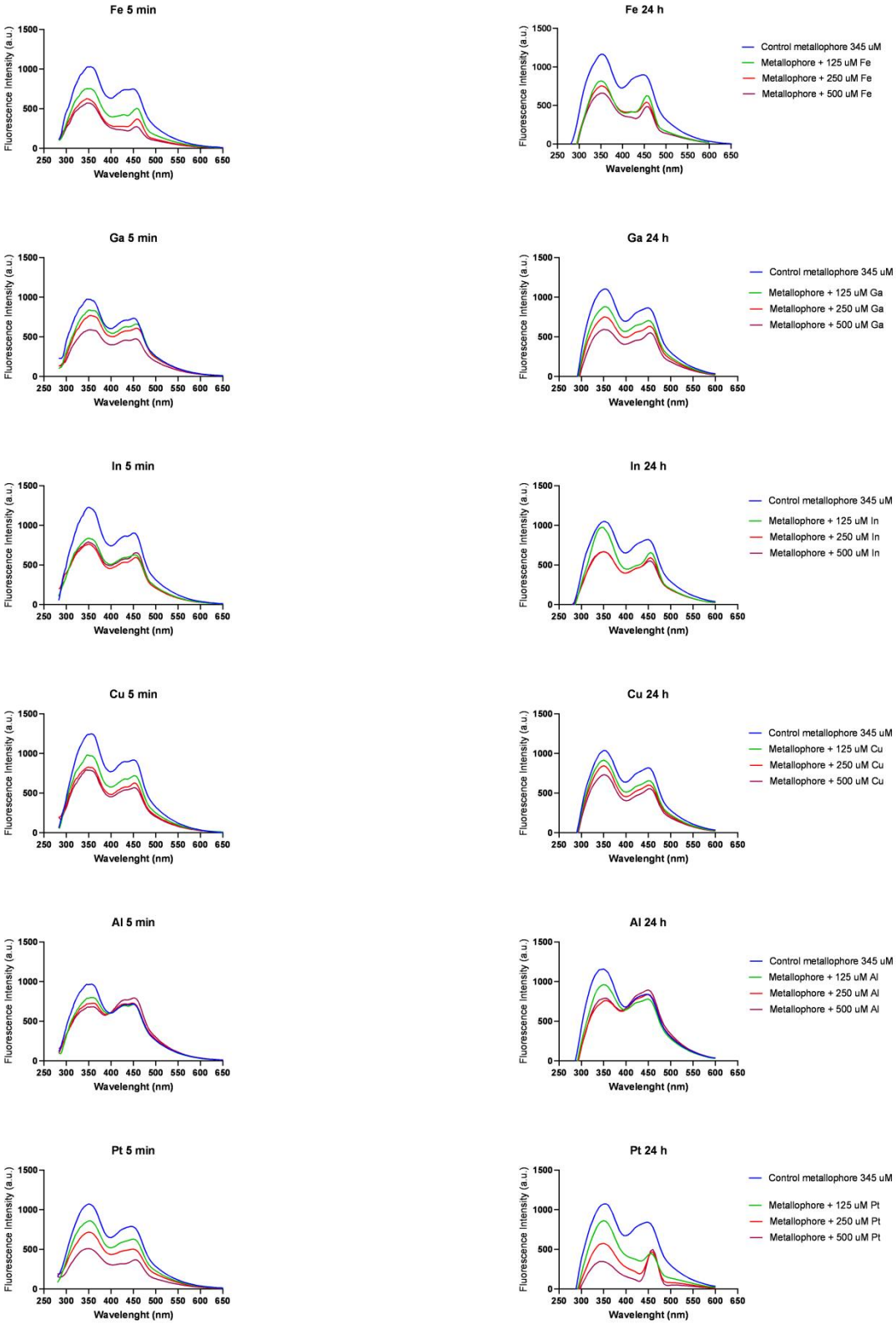

Figure 20 - Fluorescent emission spectra of metallophore produced by *P. peli* FBO M7 R9A incubated in the presence of 6 different metals. Three different concentrations of each metal were used and the fluorescent emission spectra were obtained after 5 minutes and 24 hours of incubation at room temperature.

c) *S. fonticola* A3-242

Cathecol-type metallophore purified from *S. fonticola* A3-242 with a concentration of 38 µM shows a fluorescence emission spectrum with 2 maximum fluorescence peaks, one between 325 and 330 nm and the other at 405 nm (Figure 21 and 22). Among the REEs tested Sc was the only metal capable of significantly change the fluorescence spectrum. In a concentration of 50 µM of Sc, a reduction in FI of 24.4 and 7.0 % was identified in the first and second peaks, respectively (figure 21). In general, for all REEs elements tested there were no changes in the 24-hour spectra when compared with the spectra obtained with 5 min of incubation. Regarding the remaining metals, in the case of Fe, it is observed that the first peak of the spectra of 50 and 75 µM metal at 5 minutes have similar FI. In the 24h spectrum, the spectra with metal are all similar and a reduction in FI of 16.0 and 19.4% is identified, in the first and second peaks, respectively (Figure 22). With Ga, a gradual reduction in FI is observed with increasing metal concentration in the first peak of the 5 min. In the 24-hour spectra, an FI reduction of 23.7 and 10.7 % was identified in the first and second peaks for all metal concentration tested. With In, at 5 minutes, an increase in FI is observed in the second peak with 25 µM metal. At 24 hours, a reduction is observed in all spectra with metal, reaching a reduction of 9.1 and 13.0% at 75 µM In. The presence of Pt showed a gradual decrease in FI that was correlated with the increasing metal concentration, reaching a reduction of 48.7 and 38.4 %, in the first and second peaks, respectively, with 75 µM of this metal (Figure 22). There was no change in the 24-hour spectra.

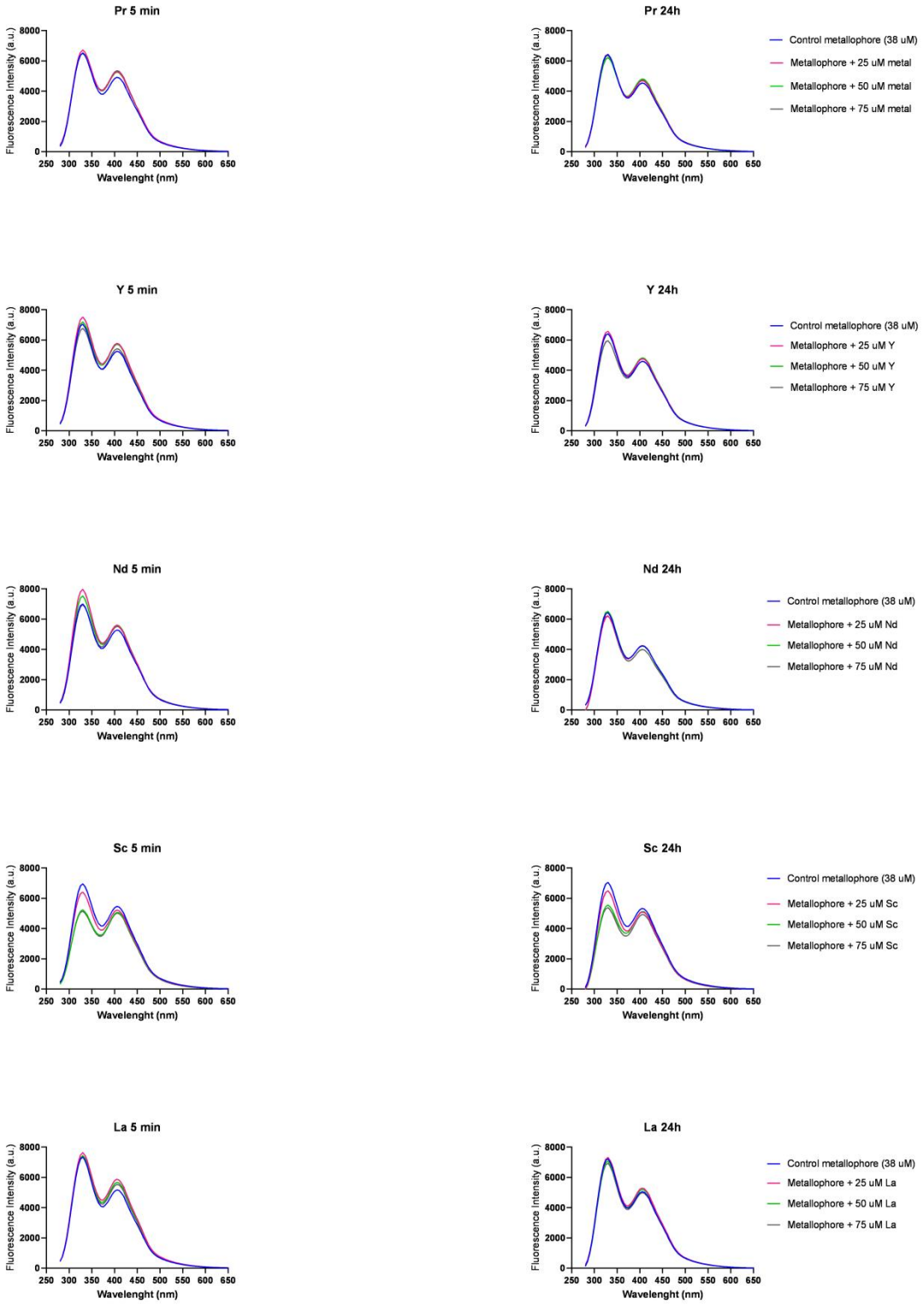

Figure 21 - Fluorescent emission spectra of metallophore produced by *S. fonticola* A3-242 incubated in the presence of 5 rare earth elements. Three different concentrations of each rare earth element were used and the fluorescent emission spectra were obtained after 5 minutes and 24 hours of incubation at room temperature.

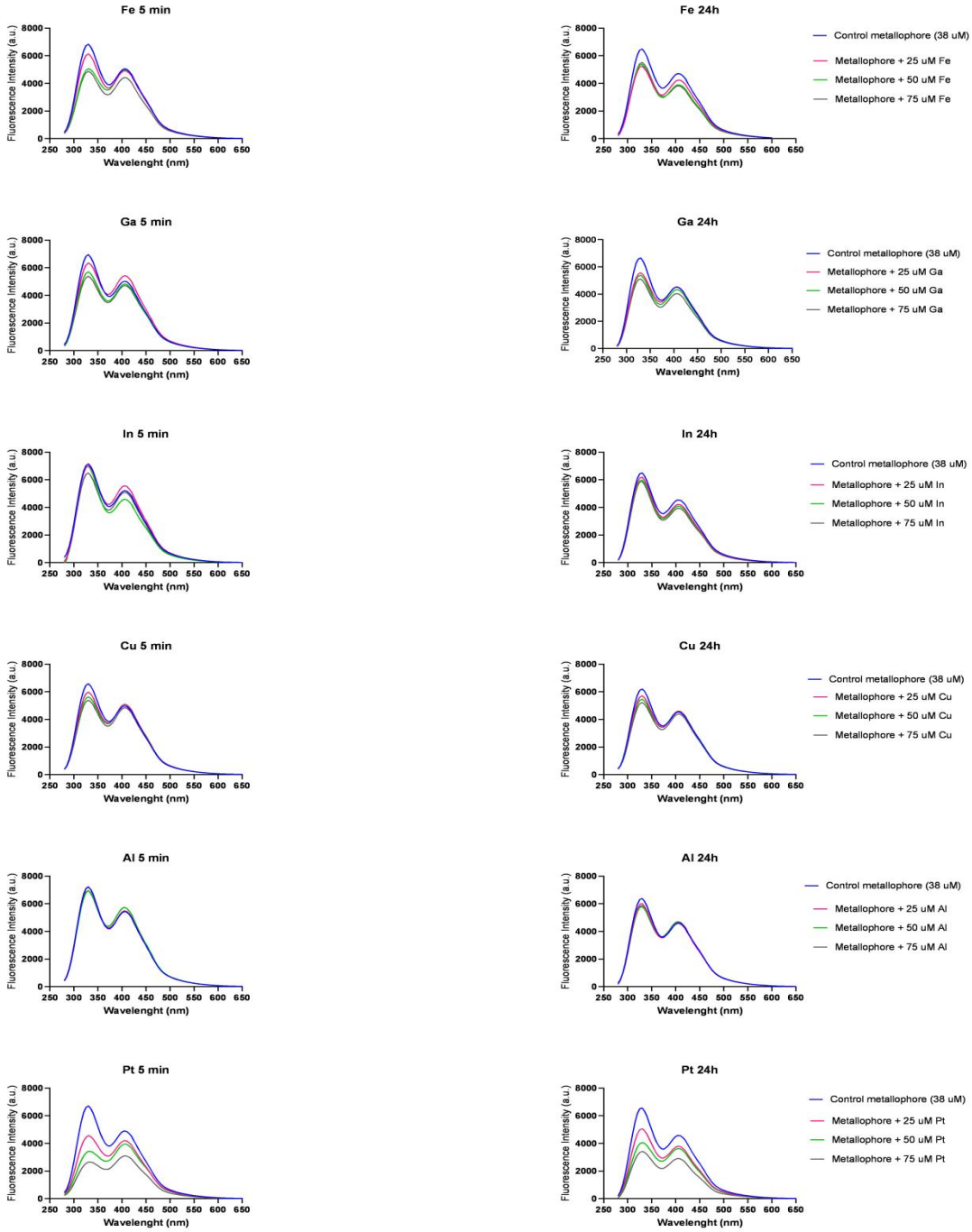

Figure 22 - Fluorescent emission spectra of metallophore produced by *S. fonticola* A3-242 incubated in the presence of 6 different metals. Three different concentrations of each metal were used and the fluorescent emission spectra were obtained after 5 minutes and 24 hours of incubation at room temperature.

DISCUSSION

The increasing demand for several metals including REEs for our current lifestyle urges the development of novel strategies to obtain those elements from secondary sources like mine residues, low-concentrated solutions from waste streams, or processing industries. Metallophores have high metal binding ability and have a high potential for application in the recovery of valuable metals. In this sense, it is of great importance to identify suitable metallophores and investigate options for their efficient use.

In this work, bacteria isolated from metal stressed environments such as mines: Navarra mine (magnesium), Jales mine (gold), Pansaqueira mine (tungsten), and Urgeiriça mine (uranium) and also a water treatment plant of a leather industry that uses chromium to process the leather, were used to test their ability to produce metallophores. These metal-contaminated environments are colonized by microbial communities well adapted to these harsh conditions, displaying several metal resistance mechanisms including the change of the metal redox state, metal cell impermeability, secretion of metal chelating agents (metallophores) to the environment, metal sorption on the microbial surface, and metal efflux (Srivastava *et al.*, 2013). In fact, of the 19 bacterial strains tested, five were able to produce metallophores to sequester metals present in the BAM CAS solid culture medium, *Ochrobactrum* sp. 5bvl1, *Bacillus altitudinis* 3w19, *Pseudomonas peli* FBO M7 R9A, *Diaphorobacter polyhydroxybutyrativorans* B2A2W2 and *Serratia fonticola* A3-242. All these isolates belong to genera where metallophore production was already reported (Martin *et al*., 2006; Dertz *et al*., 2006; Cornelis *et al.*, 2013; Schneider *et al*., 2020; Zhao *et al*., 2021). Among these isolates, *D. polyhydroxybutyrativorans* B2A2W2A and *S. fonticola* A3-242, were the ones that were able to produce metallophores that chelate all, or almost all, of the metals tested. *P. peli* FBO M7 R9A had an interesting behavior and produced metallophores only in presence of 3 REEs tested, Nd, Sc and La, and did not present growth in the BAM CAS solid medium with all other metals. This strain may be strongly affected by metal stress since bacterial growth is inhibited and the production of metallophores as a resistance mechanism against the presence of metals does not work.

Different carbon sources were used to promote bacterial growth and metallophore production. Glycerol and glucose were the carbon sources that favored the growth and production of cathecol-type metallophores in *D. polyhydroxybutyrativorans* B2A2W2A and *P. peli* FBO M7 R9A. However, *S. fonticola* A3-242, showed different growth behaviors and metallophore production depending on the agitation speed. When 140 rpm was used to agitate the culture, xylose and arabinose were the carbon sources more favorable for bacterial growth and production of cathecol-type metallophores. At 70 rpm, *S. fonticola* A3-242 showed lower bacterial growth compared to cultures incubated at 140 rpm, but produced hydroxamate-type metallophores, with glycerol and arabinose. It is well-known that medium components, such as

carbon source, and physical factors, such as temperature, dissolved oxygen, aeration and agitation greatly influence microbial growth and metabolite production (Zhou *et al*., 2018). Agitation improves both mass and oxygen transfers between the gaseous and aqueous phases and maintains homogeneous chemical and physical conditions in the medium by continuous mixing (Zhou *et al*., 2018). However, a vigorous agitation can cause shear forces, which may influence microorganisms in several ways, such as: changes in morphology, growth variation and formation of metabolites. On the other hand, low agitation reduces oxygen transfers between both phases. (Zhou *et al*. 2018) and low oxygen levels may be essential for hydroxamate-type metallophore production in *S. fonticola* A3-242. The carbon sources that most promoted the production of metallophores in these bacteria were glucose and glycerol that are widely available and have a low cost. In particular, glycerol that is a by-product of biodiesel production (Leoneti *et al*., 2012), and its use is economically viable and promotes a sustainable and a circular economy.

Although the production of both types of metallophore was feasible in this work, the metallophore purification strategy used was only effective for the purification and concentration of catechol-type metallophores. It was possible to purify and concentrate catecholate produced by *P. peli* FBO M7 R9A and *S. fonticola* A3-242 with an increase of 35 times and 23 times of the initial concentration, respectively. The hydroxamates–type metallophores produced by *S. fonticola* A3-242 with slower agitation (70 rpm) do not bind to the Amberlite resin XAD-4 and 16 used and were not eluted with the mobile phase methanol.They were soluble in the aqueous phase and were concentrated by lyophilization, nonetheless, they were lost in the process and only a small part was recovered. Thus, for future work, it is necessary to reassess the methods of purification and concentration of metallophores to adapt to the biochemical characteristics of hydroxamates.

One of the objectives of this work was to immobilize the produced hydroxamate-type metallophores in magnetic beads, and to use the immobilized magnetic beads to recover metals, including REEs, from an aqueous solution. However, this objective was not accomplished, because it was not possible to purify and concentrate the hydroxamate-type metallophore produced as was explained above. Nonetheless, the commercial DFOB was immobilized in the magnetic particles activated by 1-ethyl-3-(3-dimethylaminopropyl) carbodiimide hydrochloride (EDC). Two different concentration of DFOB was immobilized in the magnetic beads (50 mg/ml and 15 mg/ml) and both magnetic beads were used to remove Ga from 1 mM aqueous solutions of $Ga(NO_3)_3$. The percentage of Ga reduction was very similar for both beads (77-80%) and similar to the negative control, magnetic beads with EDC. Moreover, the magnetic beads by themselves were able to bind all Ga in the first 5 minutes, without the presence of immobilized metallophores. These magnetic beads have been used in previous work, also with immobilized DFOB, for Mn removal from cellulose. Only an additional 9% of Mn removal was observed with the beads with immobilized DFOB in comparison with control beads with EDC.

However, they did not use the magnetic beads alone as control (Kunz *et al*., 2020). These magnetic beads with carboxylic groups on the surface can be explored to bind and remove several metals from different solutions. However, the immobilization of metallophores onto these magnetic carriers and their use as chelating agents is currently compromised.

The metal-binding capacity of the purified metallophores was evaluated on BAM CAS agar medium. The purified catecholate-type metallophores from *P. peli* FBO M7 R9A and *S. fonticola* A3-242 were able to bind and remove all metals tested in the CAS assay. However, *P. peli* FBO M7 R9A only grew and produced metallophores in 3 REEs, Nd, Sc and La, and bacterial cells of *S. fonticola* A3-242 were not able to grow and produce metallophores in the presence of Pt. Overall, the metallophore purified from *P. peli* FBO M7 R9A forms halos with a larger diameter when compared to those formed by the metallophore from *S. fonticola* A3-242, this fact is related to a higher concentration of metallophore used in this assays. However, for both produced metallophores and also for DFOB, halos with smaller diameters were obtained with Fe, Ga and Al, and larger halos were obtained for the six REEs, In, Cu and Pt. These differences in halos sizes probably are not related to the affinity of the different metallophores towards the cations, but instead are related to the affinity of CAS for the metal. CAS probably has a higher affinity for metals such as Fe, Ga, and Al, and the different metallophores including DFOB, have more difficulty in competing with CAS for these metals and form halos with minor dimensions (Ahrens, 1952). DFOB has different affinity constants depending on the ion, and an important factor for these differences is the size of the ionic radius of the cations. However, DFOB, shows halos with the same diameter for ions such as lanthanides and Pt, with different ionic radii and electronic configurations, corroborating this fact (Ahrens, 1952).

Both produced cathecol-type metallophores showed characteristic fluorescence emission spectra, with 2 maximum fluorescence peaks, one between 350 and 355 nm and the other between 450 and 455 nm for *P. peli* FBO M7 R9A, and for *S. fonticola* A3-242 one of the spectra had peak between 325 and 330 nm and other at 405 nm. The second peak of the fluorescence emission spectra of *P. peli* FBO M7 R9A is similar to the typical fluorescence emission at 450 nm of pyoverdine I (Pvdl) a siderophore produced by *Pseudomonas aeruginosa* PAOl (Schalk *et al*., 2020; Braud *et al*., 2009). PvdI contains a fluorescent chromophore deriving from a dihydroxyquinoline. Its chemical structure also show three binding moieties including a catechol and two hydroxamates, forming with Fe^{3+} a complex with an octahedral geometry (Braud *et al*., 2009). PvdI is able to chelate, in addition to Fe^{3+}, other metals, such as Al^{3+}, Cu^{2+} and Ga^{3+}. In their work, Braud and collaborators (2019) identified total fluorescence quenching when added Fe^{3+} or Cu^{2+} to PvdI and partial quenching when Ag^{+} was added to the siderophore, indicative of the formation of PvdI–Fe, PvdI–Cu and PvdI–Ag complexes. In the remaining metals tested, there was an increase in fluorescence in the band of $\lambda = 450$ nm, which was also explained by the presence of PvdI-metal complexes or by the presence of a mixture of free PvdI and PvdI-metal (Braud *et al*., 2009). The only biochemical characterization that both

produced metallophores have, is that they belong to the catechol-type of metallophores. The chemical structure or composition of the produced metallophores is not known. However, based on the work with pyoverdine it can be assumed that the variation of FI, quenching or an increase in fluorescence, in presence of metals, shows and interaction or formation of a complex between the produced metallophores and metal.

In general, no significant changes were identified between the fluorescence spectra collected at 5 minutes and after 24 hours of interaction. Thus, the binding between metallophores and metal and the consequent formation of complexes is a process that occurs rapidly in the first minutes of interaction.

The ionic radius of the cation is a key point for the interaction and binding between the metallophores and metal (Christenson *et al.,* 2011). Table 1 shows the ionic radii of metals in hex-coordinated complexes and the electronic configuration of the cations studied in this work.

Table 7 – Ionic radii of metals. Adapted from Ahrens, 1952

	Cation	Ionic radius (Å)
REEs	Pr^{3+}	0.99
	Y^{3+}	0.90
	Nd^{3+}	0.98
	Sc^{3+}	0.75
	La^{3+}	1.03
Other metals	Fe^{3+} (high spin)	0.65
	Ga^{3+}	0.62
	In^{3+}	0.80
	Cu^{2+}	0.73
	Al^{3+}	0.54
	Pt^{4+}	0.63

The fluorescence emission spectra obtained for cations with ionic radii similar to Fe^{3+} (high spin), as is the case with Ga^{3+}, In^{3+}, Cu^{2+}, Al^{3+}, Pt^{4+} and Sc^{3+}, total or partial fluorescence quenching was observed, associated with the formation of metallophore-metal complexes. In the case of REEs that have a large ionic radius, greater than Fe^{3+}, (Pr^{3+}, Y^{3+}, Nd^{3+} and La^{3+}), this makes them too bulky for coordination with metallophores, resulting in low binding affinity and complex formation (Christenson *et al.,* 2011). Thus, the assays show little or no reduction in FI. Although it was reported logarithmic values of the stability constants between DFOB and lanthanides ranged between 10 to 15 units (Christenson *et al.,* 2011), it was not possible to identify the formation of these complexes under our condition assays.

CONCLUSIONS

- The stress caused by the presence of metal, the carbon source and agitation speed influence bacterial growth and the production of metallophores.
- Glycerol and glucose are the carbon sources that promote the bacterial growth and the production of metallophores in *Pseudomonas peli* FBO M7 R9A.
- Increased bacterial growth causes acidification of the culture medium of *Pseudomonas peli* FBO M7 R9A.
- Lower agitation speed and consequently lower oxygenation of the culture medium promotes the production of hydroxamate-type metallophores in *Serratia fonticola* A3-242.
- The mixture of resins of Amberlite XAD-4 and 16 was efficient for purifying catecholates but not hydroxamates.
- The purification process using FPLC and the mixture of resins of Amberlite XAD-4 and 16 preserves the chelating properties of the catecholate-type metallophores.
- Even though *Pseudomonas peli* FBO M7 R9A was able to form colonies and halos in only 3 (Nd, Sc and La) of the 12 metals tested, their purified catecholate-type metallophores were able to quelate all 12 metals present in the BAM CAS solid medium.
- Magnetic particles without EDC were effective at chelating metal cations.
- There was a reduction in the chelation capacity of metal cations with magnetic particles activated with EDC and DFOB immobilized in magnetic particles.
- In fluorescence assays, the interaction metallophore-metal occurs in the first 5 minutes of incubation and the ability of the metallophores to chelate the metal depends on the ionic radius of the metal cation.
- It was observed a partial quenching when commercial DFOB was incubated in the presence of Y^{3+}.
- The ionic radius of Sc^{3+} is the smallest amongst the REE and therefore the closest to Fe^{3+}. It was observed a total quenching when Sc^{3+} was incubated with commercial DFOB in 1:1 proportion. A partial quenching was observed when Sc^{3+} was incubated in the presence of purified metallophores of *P. peli* FBO M7 R9A and *S. fonticola* A3-242.
- The quenching observed in the presence of Pt^{4+} is more pronounced than with Fe^{3+} in all 3 metallophores tested.

REFERENCES

Ahrens, L. H. Geochim. Cosmochim. Acta, 2, Pages 155-169 (1952).

Albelda-Berenguer, M., Monachon, M. & Joseph, E. *Siderophores: From natural roles to potential applications*. *Advances in Applied Microbiology* vol. 106 (Elsevier Inc., 2019).

Alberti, G., Quattrini, F., Colleoni, R., Nurchi, V. M. & Biesuz, R. Deferoxamine-paper for iron (III) and vanadium(V) sensing. *Chem. Pap.* **69**, 1024–1032 (2015).

Alexander, B. & Zuberer, D. A. Use of chrome azurol S reagents to evaluate siderophore production by rhizosphere bacteria. *Biol Fertl Soils* **12**, 39–45 (1991).

Bellotti, D. & Remelli, M. Deferoxamine b: A natural, excellent and versatile metal chelator. *Molecules* **26**, 1–21 (2021).

Berraho, E. L., Lesueur, D., Diem, H. G. & Sasson, A. Iron requirement and siderophore production in Rhizobium ciceri during growth on an iron-deficient medium. *World J. Microbiol. Biotechnol.* **13**, 501–510 (1997).

Biesuz, R. *et al.* Novel DFO-SAM on mesoporous silica for iron sensing. Part I. Synthesis optimization and characterization of the material. *Analyst* **139**, 3932–3939 (2014).

Bioactivity of Serratiochelin A, a Siderophore Isolated from a Co-Culture of *Serratia* sp. and *Shewanella* sp. *Microorganisms*, *8*, 1042.

Braud, A., Hoegy, F., Jezequel, K., Lebeau, T. & Schalk, I. J. New insights into the metal specificity of the Pseudomonas aeruginosa pyoverdine-iron uptake pathway. *Environ. Microbiol.* **11**, 1079–1

Braud, A., Jézéquel, K., Bazot, S. & Lebeau, T. Enhanced phytoextraction of an agricultural Cr- and Pb-contaminated soil by bioaugmentation with siderophore-producing bacteria. *Chemosphere* **74**, 280–286 (2009).

Cezard, C., Farvacques, N. & Sonnet, P. Chemistry and Biology of Pyoverdines, Pseudomonas Primary Siderophores. *Curr. Med. Chem.* **22**, 165–186 (2014).

Christenson, E. A. & Schijf, J. Stability of YREE complexes with the trihydroxamate siderophore desferrioxamine B at seawater ionic strength. *Geochim. Cosmochim. Acta* **75**, 7047–7062 (2011).

Cornelis, P., Dingemans, J. (2013). Pseudomonas aeruginosa adapts its iron uptake strategies in function of the type of infections. Front. Cell. Infec. Microbiol., 14, DOI=10.3389/fcimb.2013.00075.

Cśaky, T. Z. On the estimation of bound hydroxylamine in biological materials. Acta Chem Scand 2:450–454 (1948).

Diels, L., Van Roy, S., Taghavi, S. & Van Houdt, R. From industrial sites to environmental applications with Cupriavidus metallidurans. *Antonie van Leeuwenhoek, Int. J. Gen. Mol. Microbiol.* **96**, 247

EIP. *European Commission, EIP, on Raw Materials, Raw Materials Scoreboard 2021*. (2021).

Gauß, R. *et al.* Rare earth magnets and motors: A European call for action. A report by the Rare Earth Magnets and Motors Cluster of the European Raw Materials Alliance. (2021).

Hermanson, G. T. Bioconjugate Chemistry - Chap 14 - Microparticles and Nanoparticles. *Bioconjug. Chem.* 582–626 (2008).

Hermanson, G. T. Zero-Length Cross-linkers. *Bioconjugate Tech.* 169–186 (1996).

Hider, R. C. & Kong, X. Chemistry and biology of siderophores. *Nat. Prod. Rep.* **27**, 637–657 (2010).

Hofmann, M., Retamal-Morales, G. & Tischler, D. Metal binding ability of microbial natural metal chelators and potential applications. *Nat. Prod. Rep.* **37**, 1262–1283 (2020).

Holden, V. I. & Bachman, M. A. Diverging roles of bacterial siderophores during infection. *Metallomics* **7**, 986–995 (2015).

Huang, X., Zhang, W., Han, S., Yin, Y., Xu, G., Wang, X. (1997). Spectrophotometric determination of Sb(III) in Sb(III)/Sb(V) binary mixtures using sodium dodecylsulfate/nonylphenoxy polyethoxyethanol mixed micellar media. Talanta: The International Journal of Pure and Applied Analytical Chemistry 45: 127-135.

Johnston, C. W. *et al.* Gold biomineralization by a metallophore from a gold-associated microbe. *Nat. Chem. Biol.* **9**, 241–243 (2013).

Khan, A., Singh, P. & Srivastava, A. Synthesis, nature and utility of universal iron chelator – Siderophore: A review. *Microbiol. Res.* **212**–**213**, 103–111 (2018).

Kinaird, J. A. & Nex, P. A. M. Critical raw materials. *Routledge Handb. Extr. Ind. Sustain. Dev.* 13–33 (2022).

Krewulak, K. D. & Vogel, H. J. Structural biology of bacterial iron uptake. *Biochim. Biophys. Acta - Biomembr.* **1778**, 1781–1804 (2008).

Kunz, P. M. *et al.* Improving manganese circular economy from cellulose by chelation with siderophores immobilized to magnetic microbeads. *Environ. Dev. Sustain.* **23**, 8252–8271 (2021).

Kurth, C., Kage, H. & Nett, M. Siderophores as molecular tools in medical and1122environmental applications. *Org. Biomol. Chem.* **14**, 8212–8227 (2016).

Leoneti, A. B., Aragão-Leoneti V., Oliveira, S. V. (2012). Glycerol as a by-product of biodiesel production in Brazil: Alternatives for the use of unrefined glycerol. Renew. Energy, 45, 138-145.

Martin, J.D., Ito, Y., Homann, V.V. *et al.* (2006). Structure and membrane affinity of new amphiphilic siderophores produced by *Ochrobactrum* sp. SP18. *J Biol Inorg Chem* 11**,** 633–641.

Matzanke, B. F. *CRC handbook of microbial iron chelates*. *Handbook of Microbial IronChelates (1991)* (1991).

Modi, M., Shah, K. S. & Modi, V. V. Isolation and characterisation of catechol-like siderophore from cowpea Rhizobium RA-1. *Arch. Microbiol.* **141**, 156–158 (1985).

Mohwinkel, D., Kleint, C. & Koschinsky, A. Phase associations and potential selective extraction methods for selected high-tech metals from ferromanganese nodules and crusts with siderophores. *Appl. Geochemistry* **43**, 13–21 (2014).

Proença, D. N. *et al.* Bacterial Metabolites Produced Under Iron Limitation Kill Pinewood Nematode and Attract Caenorhabditis elegans. *Front. Microbiol.* **10**, 1–16 (2019).

Raymond, K. N., Allred, B. E. & Sia, A. K. Coordination Chemistry of Microbial Iron Transport. *Acc. Chem. Res.* **48**, 2496–2505 (2015).

Rioux, C., Jordan, D. C. & Rattray, J. B. M. Colorimetric determination of catechol siderophores in microbial cultures. *Anal. Biochem.* **133**, 163–169 (1983).

Sayyed, R. Z. & Chincholkar, S. B. Purification of siderophores of Alcaligenes faecalis on Amberlite XAD. *Bioresour. Technol.* **97**, 1026–1029 (2006).

Schneider, Y. *et al.* Bioactivity of serratiochelin a, a siderophore isolated from a co-culture of serratia sp. and shewanella sp. *Microorganisms* **8**, 1–17 (2020).

Schwyn, B. & Neilands, J. B. Universal chemical assay for the detection and determination of siderophores. *Anal. Biochem.* **160,** 47–56 (1987).

Srivastava, P., and Kowshik, M. (2013). Mechanisms of metal resistance and homeostasis in Haloarchaea. *Archaea* 2013, 732864. doi:10.1155/2013/732864.

Stintzi, A, Raymond, K. N. (2006). Bacillibactin-Mediated Iron Transport in Bacillus subtilis. . *Am. Chem. Soc.* 128, 22–23.

Touma, Jad G. Reversible Covalent Immobilization of Desferrioxamine B (DFOB) on Aminated Polystyrene Beads for Citrate-Bound Fe(III) Chelation. (2018)

Tung, R. H. Development of effective and efficient operations for NASA's Soil Moisture Active Passive mission. *IEEE Aerosp. Conf. Proc.* 2016-June, (2016).

Turner, R. J., Weiner, J. H. and Taylor D. E. (1992). Use of diethyldithiocarbamate for quantitative determination of tellurite uptake by bacteria. Anal. Biochem. 204: 292-295.

Weakland, D. R., Smith, S. N., Bell, B., Tripathi, A. & Mobley, H. L. T. The serratia marcescens siderophore serratiochelin is necessary for full virulence during bloodstream infection. *Infect. Immun.* **88**, 1–16 (2020).

Zhao, H., Gu, Y., Liu, X., Liu, J., Waigi, MG. (2021). Reducing Phenanthrene Contamination in *Trifolium repens* L. With Root-Associated Phenanthrene-Degrading Bacterium *Diaphorobacter* sp. Phe15. Front Microbiol. Nov 26; 12:792698. doi: 10.3389/fmicb.2021.792698.

Zhou, Y. *et al.* Effects of agitation, aeration and temperature on production of a novel glycoprotein gp-1 by streptomyces kanasenisi zx01 and scale-up based on volumetric oxygen transfer coefficient. *Molecules* **23**, 1–14 (2018).